THE HARVARD-SMITHSONIAN REFERENCE ATMOSPHERE

O. GINGERICH, R. W. NOYES, and W. KALKOFEN

Smithsonian Astrophysical Observatory and Harvard College Observatory, Cambridge, Mass., U.S.A.

and

Y. CUNY

Observatoire de Paris, Section d'Astrophysique, Meudon, France

(Received 31 December, 1970)

Abstract. We present a model of the solar atmosphere in the optical depth range from $\tau_{5000} = 10^{-8}$ to 25. It combines an improved model of the photosphere that incorporates recent EUV observations with a new model of the quiet lower chromosphere. The latter is based on OSO 4 observations of the Lyman continuum, on infrared observations, and on eclipse electron densities.

Our model differs from the Bilderberg Continuum Atmosphere (BCA) in the low chromosphere ($\tau_{5000} < 10^{-4}$), where deviations from local thermodynamic equilibrium in hydrogen and carbon have been taken into account. It also differs in the transition region between the chromosphere and the photosphere ($10^{-4} < \tau_{5000} < 10^{-2}$), where the temperature is lower than in the BCA, and in the convective region ($\tau_{5000} \gtrsim 2$), where the temperature is higher than in the BCA.

1. Introduction

Empirical solar model atmospheres have traditionally used limb-darkening measurements as the means for probing different layers of the Sun's atmosphere, but a far more powerful technique became available with the advent of absolute-intensity determinations over a wide wavelength region. Because of the large opacity in the infrared and ultraviolet, the solar temperature structure can be examined through the temperature minimum and into the low chromosphere by means of continuum observations alone. One model to exploit this procedure extensively was the Bilderberg Continuum Atmosphere (Gingerich and de Jager, 1968), hereafter referred to as the BCA model. Since the time it was prepared, critical new observations have been obtained from above the earth's atmosphere, and these permit a significant improvement of the BCA model.

Rocket observations obtained in September 1968 by Parkinson and Reeves (1969) and again in 1970 include the particularly interesting ultraviolet region around 1650 Å, where the radiation arises from the coolest layers of the solar atmosphere. The brightness temperature they obtain there is below 4400 K, in contrast to the 4600 K minimum of the BCA. Their measured brightness temperature is also about 300 K below that measured by Widing *et al.* (1970); this difference corresponds to a factor of 3 change in absolute intensity. The source of the discrepancy is not yet determined.

However, independent evidence for a lower temperature minimum has been reported by Eddy *et al.* (1969b). Their airborne observations made at about 300 μ yield a brightness temperature of about 4300 K. The limb-darkening observations

Solar Physics **18** (1971) 347–365.

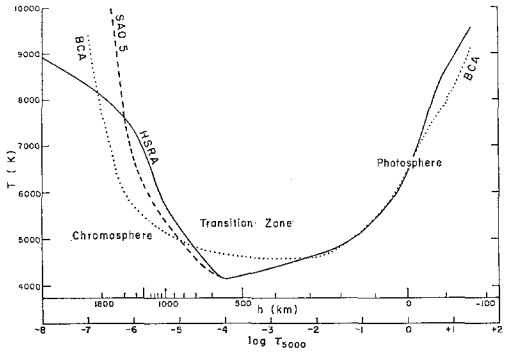

Fig. 1. Variation of temperature with optical depth τ_{5000} for three model solar atmospheres. The physical depth scale h (km) is the height above $\tau_{5000} = 1$ for the HSRA model.

of Léna (1970) at 10 μ and 20 μ provide additional evidence in this direction. Furthermore, analysis of the H and K line profiles seems to demand a lower temperature minimum, near 4300 K (Linsky and Avrett, 1970).

In light of these new observations, a preliminary revision of the BCA, calculated entirely with the assumption of local thermodynamic equilibrium (LTE), was presented at the Pasadena Solar-Physics Meeting of the American Astronomical Society in February 1969, and copies of that model, known as SAO 5, were distributed to a few investigators. It represented an attempt to drive to its ultimate limit a single-stream, LTE solar model. The Harvard-Smithsonian Reference Atmosphere (HSRA), shown in Figure 1, is a somewhat improved version. It differs from the SAO 5 for layers above $\tau_{5000} = 10^{-3}$; in this model, the temperature minimum is slightly deeper, the low chromospheric temperatures have been adjusted in the light of Cuny's (1971) non-LTE calculations, and the temperature in the chromospheric layers above $\tau_{5000} = 10^{-5}$ has been determined by Noyes and Kalkofen (1970) with the hydrogen populations in statistical equilibrium (non-LTE).

The BCA was characterized by a broad temperature plateau extending from $\tau_{5000} = 10^{-2}$ to $10^{-4.5}$; this seemed necessary in order to reproduce the observed absence of limb brightening or darkening around 1650 Å. However, the gentle downward temperature gradient of the present model still agrees with the rather qualitative center-to-limb observations around 1650 Å. In this model, the temperature minimum is reached only at $\tau_{5000} = 10^{-4}$, and the minimum zone is so narrow that its radiation cannot be investigated independently of the hotter surrounding layers. In other words, the actual minimum of 4170 K is a somewhat arbitrary choice, not well determined (see Figure 1).

The HSRA differs from the BCA in another important respect. In the deepest layers, where the model is convectively unstable, this model has temperatures several hundred degrees hotter, consistent with a mixing-length theory of convection. The problem of establishing these temperatures is intimately connected with the difficult and unresolved question of the ultraviolet opacity; it will be discussed in Section 4B.

In the remainder of this paper we discuss the observational data that have led us to

this new reference model. The details of the model are given in several tables, which appear at the end of the paper.

We wish to emphasize that the HSRA, like all models that have preceded it, should not be interpreted as an accurate description of the true solar atmosphere. The model describes an idealized plane-parallel homogeneous atmosphere in hydrostatic equilibrium; however, it is well known that in the Sun, and especially in the chromosphere, perturbations due to magnetic and hydrodynamic effects grossly distort the local structure from its mean configuration.

In addition, we expect this model, like the BCA and the Utrecht Reference Photosphere that preceded it, to be relatively short-lived. For example, new observations and analyses in the ultraviolet and infrared can be counted on to improve the mean structure in the chromospheric layers, and to shed light on inhomogeneities. Nevertheless, we hope the HSRA, in spite of its imperfections, will provide a useful framework for future improvements.

2. The Temperature Minimum Region

A. THE NATURE OF THE SOLAR SPECTRUM FROM 1500 Å TO 1800 Å

The ultraviolet solar spectrum can be divided into three distinct regions:

$\lambda > 1683$ Å	Photospheric
1683 Å $> \lambda >$ 1525 Å	Photosphere-chromosphere transition zone
1525 Å $> \lambda$	Chromospheric

Longward of 1683 Å (corresponding to the absorption edge from the ^1D first excited level of silicon), there is extremely heavy line absorption, mainly from Fe, Si, and CO. Recent photoelectric scans obtained by Parkinson and Reeves (1970) from a rocket-borne spectrometer dramatically reveal this blanketing; preliminary inspection has created a strong impression not only that 'windows' or continuum will be impossible to find, but that the average highest points are depressed far below the continuum, possibly by an order of magnitude.

The spectrum between 1683 Å and 1525 Å (the silicon ^3P ground-state edge, in emission) presents an entirely different appearance from the region longward of 1683 Å. The absolute intensity is lower, and the variations are smaller (except for the strong chromospheric emission lines primarily of C I, C IV, and Fe II). No atomic absorption lines are found here; an interesting test example is Si I, where multiplet 27 (longward of the opacity discontinuity) is in absorption, but multiplet 18 (shortward of the discontinuity) is found in emission (Parkinson and Reeves, 1970). The nature of the temperature run in the present model is consistent with the absence of atomic absorption lines in this spectral region. All easily ionized species such as Al I or Na I, which would be relatively abundant in the temperature minimum zone, have their ultimate lines and ground-state absorption edges redward of the ^1D Si limit at 1683 Å. The principal neutral lines falling between 1683 Å and 1525 Å are those of Fe I (with its edge at 1580 Å) and of Si I (with its ^3P edge bounding the region at 1525 Å). These species are more difficult to ionize, and therefore they persist into the higher temper-

atures of the low chromosphere. The known lines tend to be strong; hence, they tend to be formed in the chromosphere, and consequently they may actually appear in emission.

A contrary situation exists for carbon monoxide. The formation of CO is very sensitive to pressure, and hence CO rapidly vanishes with the diminished pressures in the low chromosphere. (In spite of its high dissociation energy, its greatest abundance occurs not at the temperature minimum itself but somewhat deeper, near $\tau_{5000}=0.03$. This explains why a temperature minimum lower than that of the BCA is still compatible with the observed CO line strengths: the temperature minimum lies where the pressure is too low for significant CO formation.) Because the CO lines are formed below the temperature minimum, they are found in absorption in the spectral region near 1600 Å; however, their weakness would prevent identification except for their occurrence in rhythmic groups.

If we assume that the CO lines are formed in LTE, their presence indicates a temperature still lower than the brightness temperature of the higher spectrum points in this region – points that fall around 4400 K according to Parkinson and Reeves (1969). Therefore, we conclude that the actual temperature minimum lies lower than 4400 K; this line of reasoning was previously expounded by Widing *et al.* (1970), albeit with higher temperatures. Our finally adopted temperature minimum of 4170 K is somewhat arbitrary; what seems clear, however, is the great potential importance of the CO lines in establishing an improved temperature structure in these layers. For this reason, we have included the number density of CO per cubic centimeter, that is, N_{CO}, in the tabulation of the model (Table V).

At the ^3P ground-state edge of Si I at 1525 Å, the spectrum shows an emission edge with a brightness temperature of about 4500 K, and the solar disk exhibits limb brightening. Both features are consonant with the model; the radiation arises from the low chromosphere, and the HSRA predicts a brightness temperature of 4480 K. The entire region is interrupted by numerous chromospheric emission lines, but these dwindle in number with shorter wavelength, making the continuum increasingly easier to define.

B. THE TEMPERATURE MINIMUM IN THE INFRARED

The spectral region 20 μ to 700 μ, in which the minimum brightness temperature occurs, is essentially inaccessible from the ground, and when the BCA was constructed in 1967, no observations were available within this wavelength range. Since that time several groups have carried out high-altitude measurements (Mankin and Strong, 1969; Mankin, 1969; Eddy *et al.*, 1969b; and Gay, 1970).

The infrared region has the great advantage of a smooth and presumably well-known opacity (H^- free-free), but the intensity of the Planck radiation is comparatively insensitive to temperature in this region. This fact, combined with the rather large error bars on the available observations, has thus far prevented a precise determination of the temperature minimum from measurements in the infrared. Nevertheless, these observations provide an invaluable consistency check on the model. The

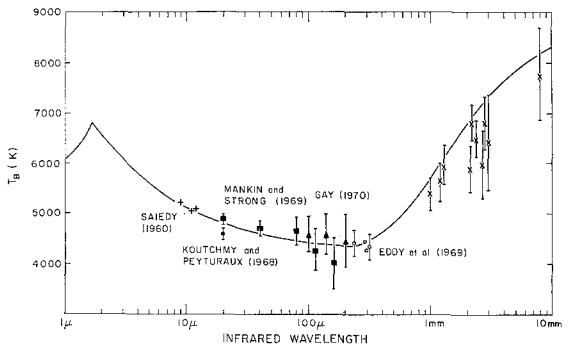

Fig. 2. Brightness temperature T_B of the disk center in the far infrared as predicted by the HSRA (solid line) and observed brightness temperatures from several authors. The crosses at wavelengths longer than 1 mm are taken from Figure 12 of Linsky and Avrett (1970), and references to the original observations are given there.

present model predicts a brightness temperature of 4390 K at 200 μ and of 4470 K at 300 μ, somewhat above the values obtained by Eddy *et al.* (see Figure 2).

This model, like the BCA before it, is comparatively poorly determined around $\tau_{5000} = 10^{-2}$. The observations of Mankin and Strong, while confirming the gradual downward temperature gradient, do not seem precise enough to require a contortion in the smooth temperature distribution of the model. The agreement with Mankin's (1969) limb darkening is reasonably satisfactory. The model predicts a change from limb darkening to brightening between 100 μ and 200 μ, and the only observation in this region that we are aware of, Mankin's at 115 μ, still shows limb darkening.

3. The Chromosphere

A. EVIDENCE FROM THE LYMAN CONTINUUM

Observations in this region of the solar spectrum were obtained in the autumn of 1967 by a Harvard College Observatory spectroheliometer aboard the OSO 4 spacecraft (Goldberg *et al.*, 1968). The observed brightness temperature at the head of the Lyman continuum is 6450 K, but the spectrum departs considerably from that of a blackbody. The continuous spectrum in this region agrees closely with that of an 8300 K blackbody whose intensity is decreased by a factor of 200; as Noyes and Kalkofen (1970) have discussed, the dilution by a factor of 200 is due to a departure from LTE.

The determination of the chromospheric temperature distribution above 6200 K in the HSRA rests primarily on these Lyman-continuum observations, but also takes into account the observed brightness temperatures in the millimeter region, the chromospheric electron densities observed at eclipse, and the height of formation of the Hα line (see Noyes and Kalkofen, 1970). The fit of the model to these several sets of observations is not perfect; rather, the model was chosen to fit all observations reasonably well, and as a result none is fit perfectly. For example, the electron density at a height 1500 km above $\tau_{5000} = 1$ lies a factor of 1.6 below that from Henze's (1969)

eclipse analysis, while the brightness temperature at 3 mm, which originates at the same height, is about 500 K higher than the mean of the observed values (Linsky and Avrett, 1970). We are unable to remove both of these discrepancies with a homogeneous model. This is no doubt due to the well-known inhomogeneous nature of the chromosphere above the temperature minimum, in particular to the chromospheric emission network and its associated spicular structure. Therefore, the model above the temperature minimum should be considered as representative of mean conditions only; it probably does not correspond in detail to the structure of any particular solar feature.

The chromospheric temperature distribution of SAO 5, a purely LTE model that satisfies the millimeter data but not the Lyman continuum, has been included in Figure 1. The difference between the SAO 5 and the BCA arises solely from an error in the BCA that came about when the chromospheric temperatures, originally on a 1-mm optical-depth scale, were transformed to τ_{5000}. The HSRA has considerably higher temperatures in the 6000 K to 7000 K range in order to produce the higher chromospheric electron densities required by the eclipse observations (Henze, 1969). To further this goal and to provide support for an overlying corona, an initial pressure of 0.15 dyne/cm^2 has been postulated (cf. Athay, 1969). As can be seen in Figure 2, the millimeter observations are only approximately satisfied, with the predicted brightness temperatures of the present model falling in the upper parts of the error bars. If the starting pressure is assumed to be zero, the agreement is much better with the millimeter observations, but the electron density is then unacceptably low.

B. EVIDENCE FROM THE ULTRAVIOLET SPECTRUM BETWEEN 912 Å AND 1525 Å

This spectral region, which includes the C and Si continua, is shown in Figure 3. Here we bridge from the Harvard rocket observations to those reduced from orbit 393 of

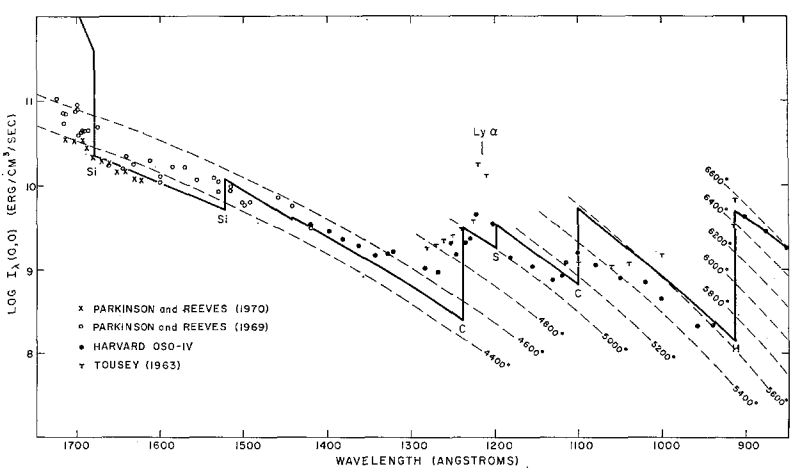

Fig. 3. Comparison of some observed EUV intensities with predictions (solid line) of the HSRA. Dashed lines are curves of constant-brightness temperature.

the OSO 4 spectrometer; the agreement between rocket and satellite data is excellent. The absolute intensities appear to be accurate within a factor of 2. Throughout this region, the continuum is comparatively easy to locate between strong chromospheric emission lines. Besides the Lyman limit, the edges from the ground state of carbon and its first excited level and from the ground state of sulfur are indicated. Both the first excited carbon edge and the sulfur edge lie in the wings of the Lyman-alpha line, and it is a moot point as to whether the S discontinuity is actually observed.

The small *T*'s in Figure 3 indicate measurements published as an upper limit by Tousey (1963). These agree with the OSO 4 data at the two C edges, but his observations were essentially limited by noise in the intervening region. The brightness temperature indicated by the OSO observations in this region lies between 5000 K and 5600 K and therefore refers to points low in the chromosphere, the very early part of the temperature rise.

In calculating the model, we took the carbon cross sections from Peach (1967) and set the sulfur ground-state cross section somewhat arbitrarily at 15 Mb (1 Mb $=10^{-18}$ cm^2). We note that Peach's quantum-defect cross section for oxygen is roughly half the hydrogenic value; the same scaling applied to the hydrogenic cross section for sulfur yields 2 Mb, in contrast to the value of 59.5 found by McGuire (1968) using Hartree-Fock-Slater parameters. More recently, Conneely *et al.* (1970) found 14 Mb with a close coupling approximation.

Cuny (1971) has shown that when the carbon ground-state continuum is calculated in non-LTE, the predicted intensity level is about 300 K lower than when calculated on the assumption of LTE. Similarly, for the first excited continuum of carbon, the depression is somewhat less than 200 K. Accordingly, the temperature distribution in the low chromosphere has been adjusted upward in the present model, so that by the LTE calculations presented here, the predicted brightness temperature is deliberately higher than that observed. We have not raised the electron temperature as much as Cuny's calculations require in order to reproduce the observed brightness temperature; however, since the uncertainty of the observations may be as high as 200 K, it seems at present futile to press for closer agreement.

4. The Photosphere

A. AGREEMENT WITH THE VISIBLE SPECTRUM

The most consistent set of solar continuum observations is without doubt that presented by Labs and Neckel (1968, 1970), but to understand the relation between their data and our model, we find it convenient to distinguish between the 'true' continuum and the 'quasi' continuum. We define the former as the intensity level of the spectrum computed with continuous opacity sources only; the numbers given in our tables refer to this true continuum. It has recently become recognized, however, that the so-called 'windows' observed in the solar ultraviolet spectrum do not coincide with this true continuum (Carbon *et al.*, 1968; Holweger, 1970); instead, there is an additional opacity produced by a veil of numerous weak lines, which we call the *haze*. Hence, we

define the quasi-continuum as the observed intensity in the most transparent windows, but lower than the true continuum because of the line haze.

Labs and Neckel give the necessary information to find the quasi-continuum in Figure 2a of their 1968 paper, where they have plotted the highest observed intensities. In their Table VI, 'the continuous spectrum of the solar center', they attempt to give the true continuum, which is, however, a model-dependent quantity in the spectral regions below about 5000 Å, where the true continuum and quasi-continuum begin to differ. Because we wish to estimate the amount of line haze predicted by this particular model, we shall need the quasi-continuum in order to compare it against the true continuum predicted by the model.

In their 1970 supplement, Labs and Neckel note the small correction required for their solar-radiation data when they adopt the International Practical Temperature Scale of 1968; this lowers the earlier values by $0.006/\lambda$, where λ is in microns. At the same time, they recognize (from Holweger's (1970) quantitative estimates of the line haze) that the true continuum and quasi-continuum differ not only below 4300 Å but even at 5000 Å, and this effect almost exactly cancels the change in the temperature scale to produce the same true continuum as before. In order for us to have the quasi-continuum, however, we shall apply the first correction only (Table I). (This procedure applies between 4300 Å and 5000 Å; below 4300 Å, the quasi-continuum must be found from their Figure 2a, with the temperature-scale correction to be applied.)

TABLE I

The continuous spectrum of the solar center (λ in microns, $I_\lambda(0)$ in W cm^{-2} ster^{-1} Å^{-1})

λ	Labs and Neckel		HSRA	HSRA	HSRA-
	True	Quasi	True	T_{Br}	L & N Quasi (%)
0.40	0.471	0.453	0.485	6559	7.0
0.42	0.462	0.454	0.472	6503	4.0
0.44	0.451	0.444	0.457	6451	2.9
0.46	0.437	0.431	0.440	6402	2.0
0.48	0.422	0.417	0.422	6357	1.3
0.50	0.407	0.402	0.408	6327	1.5
0.55	0.367	0.363	0.364	6242	0.3
0.60	0.325	0.322	0.322	6175	0.0
0.70	0.254	0.252	0.250	6081	−0.8
0.80	0.197	0.195	0.194	6031	−0.7
1.00	0.1235	0.1227	0.1218	6051	−0.7
1.20	0.0810	0.0806	0.0804	6184	−0.2
1.40	0.0563	0.0561	0.0561	6428	0.0
1.65	0.0365	0.0363	0.0367	6735	+1.1
2.00	0.0184	0.0183	0.0183	6489	0.0
2.50	0.00810	0.00807	0.00803	6229	−0.5
5.00	0.000568	0.000567	0.000562	5560	−0.9
10.00	3.69E-5	3.69E-5	3.66E-5	5107	−0.8

Table I reveals the generally excellent agreement between the photosphere of the HSRA and the observations and shows the increasing amount of haze at shorter wavelengths. Holweger tabulates 2.5% and 7.7% line absorption in windows at 5000 Å and 4000 Å, respectively, based on lines recorded in the MIT Wavelength Tables; the difference between the true continuum in the HSRA and the Labs and Neckel quasi-continuum is 1.5% and 7.0% at these wavelengths.

Table VI gives limb-darkening predictions for the HSRA. These results show gratifying agreement with observations in the visible spectrum, particularly at 4000 Å, 5000 Å, and 6000 Å, and thus meet objections raised by Elste (1968) to the BCA. The HSRA predicts far too much limb darkening in the ultraviolet region between 1683 Å and 2500 Å because of the absence of a major opacity source there, presumablys lines, as we shall discuss below.

Note added in press. Dr. Neckel points out that this procedure misinterprets their data and corrections. The Labs and Neckel (1968) Table 6 is more model-dependent than we had realized, so that the values above 0.6 μ were actually tabulated lower than the observations because of the normalization of the continuum to a model. With the correction for the International Practical Temperature Scale of 1968 and a new normalization at 6000 Å to avoid the problems of the haze at 5000 Å, the values above 6000 Å are fortuitously the same as before, and we should not have lowered them in this region to obtain the quasi-continuum. As a result, the HSRA predicts intensities generally between 1% and 2% too low in the $0.6-2.0$ μ region, although still within the observational error. According to Dr. Neckel, the intensities could be appropriately increased by a temperature rise of about 20 K in the shallower layers and 30 K at $\tau=1$. Furthermore, the discrepancy at 1.65 μ no longer suggests a lowering of the temperature in the convective zone.

B. THE CONVECTIVE ZONE

The 1% discrepancy shown in Table I at 1.65 μ, where the atmosphere is particularly transparent, suggests that the deeper layers in the convective zone of the HSRA are too hot, possibly by as much as 200 K at optical depth 10. (In comparison, the BCA is about 600 K cooler at $\tau=10$, and Elste's (1968) model is 400 K cooler at $\tau=10$.) It is difficult to establish the temperature distribution empirically at great depths; the 1.65 μ opacity window offers little leverage, since it is only twice as transparent as the 5000 Å standard. If the line-haze opacity were more quantitatively understood, the region just above the Balmer discontinuity, around 3800 Å, could provide critical evidence about the deeper layers, since the Planck function rises more rapidly here than at 16500 Å and the radiation from the hot convective layers could have a detectable influence on the emergent intensity.

Convection theory offers at least some guidance concerning the shape of the temperature distribution in the deeper layers. Carbon and Gingerich (1969) have computed a series of theoretical blanketed models with a mixing-length theory; the behavior of the convective zone in the theoretical models is quite close to that in the empirical

model given here. Again, a lowering of the temperatures at $\tau = 10$ and deeper is suggested, but only by a few score degrees.

C. THE ULTRAVIOLET FROM 3646 Å TO 1683 Å

The crowding of lines in this spectral region virtually prevents observation of the continuum. The highest intensity points, to the extent that they can be observed, constitute the quasi-continuum, which is far different from the true-continuum level given in Table VI. The disparity is strikingly shown on Figure 4, where near 1800 Å the true continuum lies more than an order of magnitude above the rocket observations of Parkinson and Reeves. *This discrepancy reflects our inadequate knowledge of the opacity and does not result from the choice of the temperature distribution, which is well determined by other spectral regions.* A detailed discussion of the difference between the true continuum and the quasi-continuum, which presumably arises from line blanketing in this region, will be the subject of a further paper. Here it will suffice to remark on the continuous-opacity sources of the model.

The aluminum ground-state cross section is taken as 22 Mb, in agreement with preliminary unpublished results from the Harvard Shock Tube Laboratory and with

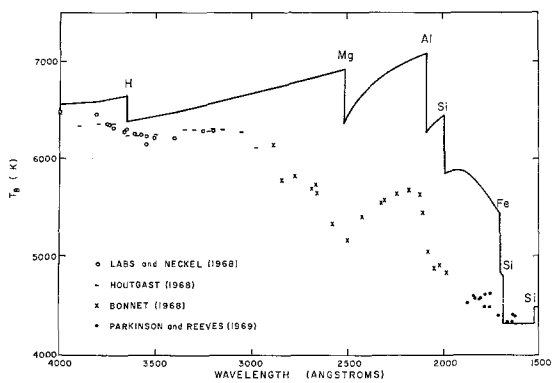

Fig. 4. Observed brightness temperatures in the ultraviolet, compared with the predictions (solid line) of the HSRA.

recent theoretical determinations. It also agrees with recent experimental results of Kozlov and Startsev (1969). We have used the higher aluminum abundance of Lambert and Warner (1968). Although the size of the observed discontinuity at 2077 Å is reproduced fairly well, it may well diminish in size when further opacity is added.

The cross section for the first excited state ($^3P^0$) of magnesium was determined experimentally by Bötticher (1958) with respect to the Mg λ3338 line; as pointed out to us by Dr. T. Simon, the gf value of that line has recently been redetermined, so that the $^3P^0$ cross section appears to be 25 instead of 45 Mb. This smaller value leads to a fairly good representation of the discontinuity at 2518 Å.

The large Si ^1D discontinuity predicted at 1683 Å has been the subject of repeated inquiry, but attempts to find a significant new continuous opacity source have thus far

failed. Doyle (1968) carried out detailed calculations on quasi-molecular hydrogen, and his absorption coefficients have been included in our model. Cuny (1969) proposed that the resonance-broadening wing of the Lyman-alpha line might have a pervasive effect throughout this entire ultraviolet region, but Sando *et al.* (1969) pointed out that for such close encounters of neutral atoms, the hydrogen essentially becomes molecular and has a band head at 1623 Å. When rotational structure is taken into account, absorption extends to longer wavelengths only over a short interval redward of 1683 Å; Sando's (1969) quantum-mechanical absorption coefficients have been used in the model in this region, but this opacity is actually negligible here. (E. H. Avrett has pointed out to us that we should not have neglected the resonance-broadening wing of the Lyman-alpha line in the wavelengths shorter than 1623 Å; when included in the form used by Cuny, it raises the continuum and produces a significantly better agreement with the observations.) We have incorporated bound-free transitions from many low-lying levels of iron; this creates a discontinuity at 1700 Å, but it does not affect the longer wavelengths. Even with the higher iron abundance proposed by Garz *et al.* (1969), this does not appear to be a very important absorber, contrary to their and our expectations (Gingerich, 1970).

Although the search for additional continuous absorbers in the ultraviolet must proceed, we believe that the principal opacity not included in the model can be attributed to the lines, perhaps in part to the veil of weak-line haze invoked to explain the near ultraviolet and in part to the wings of numerous strong and intermediate lines. As mentioned in Section 2 A, the new observations of Parkinson and Reeves (1970) lend support to this interpretation.

5. Computational Aspects

The computations shown here were carried out on a Control Data Corporation 6400 with Gingerich's stellar atmosphere program, which is the same as that used for the BCA. The program has been slightly modified to accept the departure coefficients

TABLE II

Elements entering the equation of state

Element	Relative abundance	Abundance $\log\varepsilon + 12$	Ionization potential	log $2U_{II}/U_I$
H	1.00	12.00	13.595	0.000
He	0.10	11.00	24.581	0.602
C	3.55E-4	8.55	11.256	0.110
O	5.90E-4	8.77	13.614	−0.004
Na	1.51E-6	6.18	5.138	−0.010
Mg	3.02E-5	7.48	7.644	0.600
Al	2.51E-6	6.40	5.984	−0.470
Si	3.55E-5	7.55	8.149	0.080
S	1.62E-5	7.21	10.357	0.000
Fe	3.16E-5	7.50	7.830	0.491

(b_1) for the hydrogen ground state, which were calculated by Noyes and Kalkofen (1970). This was done simply by multiplying the hydrogen partition function by b_1 in the Saha equation of state and then changing the hydrogen-opacity routine so that higher levels and the free-free absorption were not affected by the overpopulation of the ground state. The b_1 values are listed in Table V; beginning at $\tau = 0.0000158$, they have been arbitrarily taken as unity.

The He/H ratio by number is set at $\frac{1}{10}$ as in the BCA, but the abundances for the other elements except iron have been taken from Lambert and Warner (1968), as

TABLE III

Additional ultraviolet opacity routines

```
      FUNCTION AVFE(TH,FR)                                              AVFE  10
C-----HYDROGENIC APPROXIMATION FOR BOUND-FREE IRON OPACITY - 6 OCT. 69. AVFE  20
      DIMENSION WLIM(6)                                                 AVFE  30
      DATA WLIM /1570.,1680.,1700.,1730.,1815.,1860./,F/0/              AVFE  40
      IF(FR.GT.19.63E14) GO TO 7                                        AVFE  50
      TK=.43429/TH                                                      AVFE  60
      IF(FR-F) 20,24,20                                                 AVFE  70
   20 F=FR                                                              AVFE  80
      W=2.9979E18/F                                                     AVFE  90
      HVE=4.1352E-15*F                                                  AVFE 100
      F3=(F*1.E-15)**3                                                  AVFE 110
      DO 22 I=1,6                                                       AVFE 120
      IF(W.LIM(I)-W) 22,24,24                                           AVFE 130
   22 CONTINUE                                                          AVFE 140
C-----NO ABSORPTION REDWARD OF 1860A OR SHORT OF 1526A.                 AVFE 150
      I=7                                                               AVFE 160
    7 AVFE=0.                                                           AVFE 170
      RETURN                                                            AVFE 180
   24 I=I                                                               AVFE 190
      SUM=0.                                                            AVFE 200
      GO TO (1,2,3,4,5,6,7),I                                           AVFE 210
C-----COEFFICIENTS ARE CROSS SECTION IN MEGABARNS, FREQUENCY CUBED      AVFE 220
C-----SCALED DOWN BY E45. STATISTICAL WEIGHT FOR LEVEL.                 AVFE 230
    1 SUM=594.                                                          AVFE 240
    2 SUM=187./EXP(2.18/TK)+88./EXP(4.59/TK)+SUM                        AVFE 250
    3 SUM=660./EXP(0.87/TK)+SUM                                         AVFE 260
    4 SUM=278./EXP(2.70/TK)+81./EXP(3.04/TK)+394./EXP(3.26/TK)+SUM      AVFE 270
    5 SUM=80./EXP(3.06/TK)+23./EXP(3.42/TK)+114./EXP(3.56/TK)+SUM       AVFE 280
    6 SUM=328./EXP(1.49/TK)+88./EXP(2.84/TK)+SUM                        AVFE 290
      AVFE=SUM/F3*1.E8*(1.-EXP(-HV/TK))/25.                             AVFE 300
      RETURN                                                            AVFE 310
      END                                                               AVFE 320


      SUBROUTINE AVLYM(TH,FR)                                           AVLY  10
C-----OPACITY PER NEUTRAL HYDROGEN ATOM FOR RESONANCE BROADENING OF     AVLY  20
C-----LYMAN ALPHA LINE, BASED ON CALCULATIONS OF KENNETH SANDO, JULY 69.AVLY  30
      WAVE=2.9979E18/FR                                                 AVLY  40
      IF((WAVE.GT.1950.).OR.(WAVE.LT.1630)) GO TO 40                    AVLY  50
C-----O.M. TREATMENT FOR 1950A - 1630A.                                 AVLY  60
      T=5040.4/TH                                                       AVLY  70
      B=.0471+35./T                                                     AVLY  80
      AVLYM=4.03E-12/SQRT(T)*EXP(B*(1620.-WAVE))                        AVLY  90
      RETURN                                                            AVLY 100
   40 AVLYM=0.                                                          AVLY 110
      RETURN                                                            AVLY 120
      END                                                               AVLY 130


      FUNCTION AVQH2(THETA,FREQ)                                        AVQH  10
C-----AVQH2 APPROXIMATES THE QUASI-HYDROGEN MOLECULAR ABSORPTION        AVQH  20
C-----COEFFICIENTS GIVEN IN THE DOYLE THESIS, HARVARD 1968.             AVQH  30
C-----4 APRIL 1968 VERSION MUST BE MULTIPLIED BY H/CC.                  AVQH  40
C                                                                       AVQH  50
      DIMENSION FRLIM(5)                                                AVQH  60
C                                                                       AVQH  70
C---NU FOR          1665A      1875A      2100A      2350A      2750A  AVQH  80
      DATA FRLIM/18.224E14, 15.989E14, 14.278E14, 12.757E14, 10.901E14/ AVQH  90
C                                                                       AVQH 100
    4 TEMP=5.040/THETA                                                  AVQH 110
      IF(FRLIM(5)-FREQ) 15,15,5                                         AVQH 120
    5 AVQH2=0.0                                                         AVQH 130
      RETURN                                                            AVQH 140
   15 DO 20 INDEX=1,4                                                   AVQH 150
      IF(FREQ-FRLIM(INDEX)) 20,25,25                                    AVQH 160
   20 CONTINUE                                                          AVQH 170
C-----COEFFICIENT AT 1540A                                              AVQH 180
      AVQH2=79.057+(-57.532+10.191*TEMP)*TEMP                           AVQH 190
   25 GO TO (30,40,50,60),INDEX                                         AVQH 200
C-----COEFFICIENT AT 1540A                                              AVQH 210
   30 AVQH2=-1.5527E3+(2.0309E3-1.2391E2*TEMP)*TEMP                     AVQH 220
      GO TO 10                                                          AVQH 230
C-----COEFFICIENT AT 1750A                                              AVQH 240
   40 AVQH2=-2.2983E3+(1.1117E3-40.873*TEMP)*TEMP                       AVQH 250
      GO TO 10                                                          AVQH 260
C-----COEFFICIENT AT 2000A                                              AVQH 270
   50 AVQH2=-462.84+(140.64+11.809*TEMP)*TEMP                           AVQH 280
      GO TO 10                                                          AVQH 290
C-----COEFFICIENT AT 2200A                                              AVQH 300
   60 AVQH2=-24.813+(-32.570+14.373*TEMP)*TEMP                          AVQH 310
   10 AVQH2=AVQH2*1.E-19                                                AVQH 320
      RETURN                                                            AVQH 330
      END                                                               AVQH 340
```

Note: Following line AVQH 190 the statement GO TO 10 has been accidentally omitted in the reproduction copy above.

TABLE IV

Harvard-Smithsonian reference atmosphere

T EFF = 5780. LOG G = 4.440. HELIUM/HYDROGEN BY NUMBER= .100. ABUNDANCES LW=FE=7.5

OPTICAL DEPTH	TEMP (K)	PRESSURE (CGS)	ELECTRON PRESSURE	OPACITY (PER GM)	HYDROGEN IONIZED	METAL TOTAL	ELECTRON CONTRIBUTORS SI	MG	FE	C	DENSITY (GM/CC)	GRADIENT RADIATIVE	GRADIENT ADIABATIC	DEPTH (CM)
1.00E-08	8930.0	1.518E-01	4.822E-02	1.46E-01	5.11E-01	.2	.0	.0	.0	.1	1.81E-13	0.	7.43E+08	-1.85E+08
1.26E-08	8880.0	1.523E-01	4.845E-02	1.47E-01	5.12E-01	.2	.0	.0	.0	.1	1.82E-13	-2.04E+10	7.30E+08	-1.85E+08
1.58E-08	8810.0	1.529E-01	4.826E-02	1.45E-01	5.07E-01	.2	.0	.0	.0	.1	1.85E-13	-1.80E+10	7.24E+08	-1.85E+08
2.00E-08	8750.0	1.537E-01	4.838E-02	1.45E-01	5.05E-01	.2	.0	.0	.0	.1	1.88E-13	-1.41E+10	7.13E+08	-1.85E+08
2.51E-08	8680.0	1.547E-01	4.823E-02	1.43E-01	4.98E-01	.2	.0	.0	.0	.1	1.91E-13	-1.06E+10	7.06E+08	-1.84E+08
3.16E-08	8630.0	1.559E-01	4.915E-02	1.45E-01	5.06E-01	.2	.0	.0	.0	.1	1.93E-13	-8.12E+09	6.81E+08	-1.84E+08
3.98E-08	8560.0	1.575E-01	4.931E-02	1.44E-01	5.01E-01	.2	.0	.0	.0	.1	1.97E-13	-6.70E+09	6.69E+08	-1.84E+08
5.01E-08	8510.0	1.594E-01	5.028E-02	1.45E-01	5.06E-01	.2	.0	.0	.0	.1	2.00E-13	-4.74E+09	6.46E+08	-1.84E+08
6.31E-08	8450.0	1.619E-01	5.100E-02	1.45E-01	5.05E-01	.2	.0	.0	.0	.1	2.05E-13	-4.45E+09	6.27E+08	-1.83E+08
7.94E-08	8380.0	1.650E-01	5.207E-02	1.46E-01	5.07E-01	.2	.0	.0	.0	.1	2.10E-13	-3.60E+09	6.03E+08	-1.83E+08
1.00E-07	8320.0	1.689E-01	5.345E-02	1.46E-01	5.09E-01	.2	.0	.0	.0	.1	2.16E-13	-2.81E+09	5.77E+08	-1.82E+08
1.26E-07	8250.0	1.737E-01	5.514E-02	1.47E-01	5.11E-01	.2	.0	.0	.0	.1	2.23E-13	-2.58E+09	5.49E+08	-1.81E+08
1.58E-07	8170.0	1.798E-01	5.722E-02	1.48E-01	5.13E-01	.2	.0	.0	.0	.1	2.34E-13	-2.20E+09	5.17E+08	-1.80E+08
2.00E-07	8090.0	1.875E-01	5.983E-02	1.49E-01	5.02E-01	.2	.0	.0	.0	.1	2.48E-13	-1.85E+09	4.95E+08	-1.79E+08
2.51E-07	8000.0	1.973E-01	6.105E-02	1.43E-01	4.92E-01	.2	.0	.0	.0	.1	2.65E-13	-1.56E+09	4.68E+08	-1.78E+08
3.16E-07	7910.0	2.099E-01	6.438E-02	1.41E-01	4.86E-01	.2	.0	.0	.0	.1	2.87E-13	-1.24E+09	4.34E+08	-1.76E+08
3.98E-07	7820.0	2.261E-01	6.770E-02	1.37E-01	4.70E-01	.2	.0	.0	.0	.1	3.16E-13	-1.08E+09	4.06E+08	-1.74E+08
5.01E-07	7710.0	2.475E-01	7.046E-02	1.28E-01	4.37E-01	.2	.0	.0	.0	.1	3.58E-13	-8.42E+08	3.87E+08	-1.72E+08
6.31E-07	7630.0	2.762E-01	7.495E-02	1.20E-01	4.09E-01	.3	.0	.0	.0	.1	4.11E-13	-7.06E+08	3.62E+08	-1.69E+08
7.94E-07	7500.0	3.165E-01	7.652E-02	1.04E-01	3.50E-01	.3	.0	.0	.0	.1	4.99E-13	-7.38E+08	3.60E+08	-1.66E+08
1.00E-06	7360.0	3.763E-01	7.846E-02	8.63E-02	2.89E-01	.3	.0	.0	.0	.1	6.31E-13	-6.88E+08	3.59E+08	-1.62E+08
1.26E-06	7180.0	4.736E-01	7.529E-02	6.24E-02	2.07E-01	.5	.0	.0	.0	.2	8.65E-13	-6.70E+08	3.99E+08	-1.57E+08
1.58E-06	6970.0	6.512E-01	7.276E-02	4.22E-02	1.38E-01	.7	.0	.0	.0	.3	1.29E-12	-6.27E+08	4.49E+08	-1.51E+08
2.00E-06	6720.0	1.003E+00	6.847E-02	2.52E-02	7.99E-02	1.0	.0	.0	.0	.4	2.17E-12	-5.76E+08	5.45E+08	-1.43E+08
2.51E-06	6440.0	1.812E+00	6.252E-02	1.30E-02	3.87E-02	1.6	.1	.1	.1	.9	4.23E-12	-4.71E+08	7.38E+08	-1.33E+08
3.16E-06	6180.0	3.793E+00	6.002E-02	6.67E-03	1.72E-02	2.9	.2	.2	.2	1.9	9.41E-12	-3.40E+08	9.58E+08	-1.23E+08
3.98E-06	5950.0	8.225E+00	6.258E-02	4.08E-03	8.00E-03	5.3	.4	.4	.4	3.6	2.14E-11	-2.37E+08	9.74E+08	-1.12E+08
5.01E-06	5750.0	1.655E+01	6.509E-02	3.04E-03	3.97E-03	8.6	.8	.7	.7	5.7	4.47E-11	-1.59E+08	8.08E+08	-1.02E+08
6.31E-06	5590.0	2.916E+01	6.779E-02	2.69E-03	2.26E-03	11.8	1.4	1.2	1.2	7.1	8.11E-11	-1.08E+08	5.83E+08	-9.47E+07
7.94E-06	5440.0	4.611E+01	6.728E-02	2.55E-03	1.37E-03	14.8	2.2	1.9	2.0	7.5	1.32E-10	-7.99E+07	4.17E+08	-8.88E+07
1.00E-05	5300.0	6.790E+01	6.769E-02	2.58E-03	9.13E-04	16.9	3.2	2.7	2.9	6.6	1.99E-10	-5.91E+07	2.88E+08	-8.40E+07
1.26E-05	5170.0	9.649E+01	6.057E-02	2.43E-03	5.36E-04	22.5	5.1	4.4	4.6	6.5	2.91E-10	-4.50E+07	2.22E+08	-7.97E+07
1.58E-05	5040.0	1.346E+02	5.218E-02	2.26E-03	2.92E-04	31.5	8.2	7.1	7.4	6.3	4.16E-10	-3.58E+07	1.73E+08	-7.58E+07
2.00E-05	4910.0	1.866E+02	4.432E-02	2.11E-03	1.41E-04	46.2	13.4	11.5	12.0	5.9	5.92E-10	-2.75E+07	1.34E+08	-7.20E+07
2.51E-05	4790.0	2.544E+02	4.066E-02	2.10E-03	6.45E-05	63.3	19.7	17.1	17.9	4.7	8.28E-10	-2.16E+07	9.72E+07	-6.85E+07
3.16E-05	4660.0	3.375E+02	3.966E-02	2.24E-03	2.46E-05	80.9	26.3	23.3	24.2	2.9	1.13E-09	-1.79E+07	6.76E+07	-6.54E+07
3.98E-05	4530.0	4.314E+02	4.228E-02	2.59E-03	8.15E-06	92.5	30.2	27.8	28.8	1.4	1.48E-09	-1.42E+07	4.45E+07	-6.27E+07
5.01E-05	4400.0	5.307E+02	4.681E-02	3.14E-03	2.45E-06	97.5	30.5	30.6	31.4	.5	1.88E-09	-1.09E+07	2.90E+07	-6.06E+07
6.31E-05	4280.0	6.342E+02	5.198E-02	3.76E-03	7.65E-07	99.1	29.2	33.0	33.1	.2	2.31E-09	-7.07E+06	1.98E+07	-5.88E+07
7.94E-05	4200.0	7.452E+02	5.527E-02	4.33E-03	3.34E-07	99.6	25.2	35.1	34.2	.1	2.76E-09	-3.18E+06	1.43E+07	-5.72E+07
1.00E-04	4170.0	8.682E+02	6.119E-02	4.87E-03	2.26E-07	99.7	23.3	36.3	34.8	.1	3.24E-09	-6.33E+05	1.09E+07	-5.57E+07
1.26E-04	4175.0	1.007E+03	6.958E-02	5.43E-03	2.09E-07	99.7	22.6	36.8	34.9	.1	3.76E-09	3.27E+05	8.41E+06	-5.43E+07
1.58E-04	4190.0	1.163E+03	7.964E-02	6.04E-03	2.11E-07	99.7	22.3	37.0	35.0	.1	4.33E-09	4.13E+05	6.57E+06	-5.29E+07
2.00E-04	4205.0	1.340E+03	9.093E-02	6.72E-03	2.13E-07	99.7	22.0	37.2	35.0	.1	4.97E-09	3.76E+05	5.14E+06	-5.15E+07
2.51E-04	4225.0	1.541E+03	1.041E-01	7.56E-03	2.25E-07	99.7	21.9	37.3	35.0	.1	5.68E-09	3.86E+05	4.05E+06	-5.01E+07
3.16E-04	4250.0	1.768E+03	1.197E-01	8.29E-03	2.47E-07	99.7	21.9	37.2	35.0	.1	6.48E-09	3.75E+05	3.20E+06	-4.87E+07
3.98E-04	4280.0	2.026E+03	1.380E-01	9.20E-03	2.83E-07	99.6	22.2	37.0	34.9	.1	7.38E-09	3.04E+05	2.53E+06	-4.74E+07
5.01E-04	4305.0	2.319E+03	1.582E-01	1.02E-02	3.11E-07	99.6	22.2	37.0	34.9	.1	8.40E-09	2.18E+05	2.01E+06	-4.60E+07
6.31E-04	4330.0	2.651E+03	1.810E-01	1.13E-02	3.40E-07	99.5	22.3	36.9	34.9	.1	9.54E-09	1.73E+05	1.59E+06	-4.47E+07
7.94E-04	4355.0	3.028E+03	2.071E-01	1.25E-02	3.72E-07	99.5	22.3	36.9	34.8	.1	1.08E-08	1.37E+05	1.26E+06	-4.33E+07

T EFF = 5780. LOG G = 4.440. HELIUM/HYDROGEN BY NUMBER= .100. ABUNDANCES LW=FE=7.5

OPTICAL DEPTH	TEMP (K)	PRESSURE (CGS)	ELECTRON PRESSURE	OPACITY (PER GM)	HYDROGEN IONIZED	METAL TOTAL	ELECTRON CONTRIBUTORS SI	MG	FE	C	DENSITY (GM/CC)	GRADIENT RADIATIVE	GRADIENT ADIABATIC	DEPTH (CM)
.0010000	4380.0	3.457E+03	2.366E-01	1.39E-02	4.06E-07	99.5	22.3	36.8	34.8	.1	1.23E-08	1.09E+05	1.00E+06	-4.20E+07
.0012589	4405.0	3.944E+03	2.702E-01	1.54E-02	4.43E-07	99.4	22.4	36.8	34.8	.1	1.40E-08	8.66E+04	7.99E+05	-4.07E+07
.0015849	4430.0	4.497E+03	3.083E-01	1.71E-02	4.81E-07	99.4	22.4	36.8	34.7	.1	1.58E-08	7.49E+04	6.36E+05	-3.93E+07
.0019953	4460.0	5.125E+03	3.533E-01	1.89E-02	5.43E-07	99.3	22.5	36.6	34.7	.1	1.79E-08	6.56E+04	5.07E+05	-3.79E+07
.0025119	4490.0	5.839E+03	4.046E-01	2.10E-02	6.11E-07	99.2	22.7	36.5	34.6	.2	2.03E-08	5.59E+04	4.04E+05	-3.66E+07
.0031623	4525.0	6.650E+03	4.652E-01	2.32E-02	7.11E-07	99.1	23.0	36.2	34.5	.2	2.29E-08	4.22E+04	3.23E+05	-3.52E+07
.0039811	4550.0	7.571E+03	5.297E-01	2.57E-02	7.66E-07	99.0	23.0	36.2	34.4	.2	2.59E-08	2.74E+04	2.57E+05	-3.39E+07
.0050119	4575.0	8.618E+03	6.029E-01	2.85E-02	8.25E-07	98.9	22.9	36.2	34.4	.2	2.94E-08	2.18E+04	2.05E+05	-3.25E+07
.0063096	4600.0	9.807E+03	6.861E-01	3.16E-02	8.87E-07	98.8	22.9	36.1	34.4	.2	3.32E-08	1.88E+04	1.64E+05	-3.11E+07
.0079433	4630.0	1.116E+04	7.839E-01	3.50E-02	9.85E-07	98.7	23.0	36.0	34.3	.2	3.76E-08	1.65E+04	1.31E+05	-2.97E+07
.0100000	4660.0	1.269E+04	8.953E-01	3.88E-02	1.09E-06	98.6	23.1	35.9	34.2	.2	4.25E-08	1.31E+04	1.04E+05	-2.83E+07
.0125893	4690.0	1.444E+04	1.022E+00	4.30E-02	1.21E-06	98.4	23.1	35.8	34.1	.2	4.80E-08	1.04E+04	8.32E+04	-2.69E+07
.0158489	4720.0	1.642E+04	1.167E+00	4.76E-02	1.33E-06	98.3	23.2	35.6	34.0	.2	5.42E-08	8.26E+03	6.65E+04	-2.55E+07
.0199526	4750.0	1.867E+04	1.331E+00	5.28E-02	1.46E-06	98.1	23.2	35.5	33.9	.3	6.13E-08	7.53E+03	5.31E+04	-2.41E+07
.0251189	4790.0	2.122E+04	1.532E+00	5.85E-02	1.71E-06	97.8	23.5	35.2	33.8	.3	6.91E-08	7.72E+03	4.25E+04	-2.27E+07
.0316228	4840.0	2.412E+04	1.777E+00	6.49E-02	2.13E-06	97.4	23.9	34.7	33.4	.3	7.77E-08	7.20E+03	3.40E+04	-2.12E+07
.0398107	4895.0	2.742E+04	2.069E+00	7.20E-02	2.71E-06	96.7	24.3	34.0	33.0	.4	8.73E-08	6.03E+03	2.73E+04	-1.98E+07
.0501187	4950.0	3.116E+04	2.408E+00	7.99E-02	3.43E-06	96.0	24.7	33.4	32.6	.4	9.81E-08	4.98E+03	2.19E+04	-1.83E+07
.0630957	5010.0	3.540E+04	2.814E+00	8.87E-02	4.43E-06	94.9	25.0	32.6	32.1	.5	1.10E-07	4.45E+03	1.76E+04	-1.68E+07
.0794328	5080.0	4.020E+04	3.317E+00	9.87E-02	6.01E-06	93.4	25.3	31.6	31.3	.6	1.23E-07	4.09E+03	1.41E+04	-1.53E+07
1.000000	5160.0	4.562E+04	3.950E+00	1.10E-01	8.49E-06	91.1	25.3	30.3	30.2	.8	1.38E-07	3.49E+03	1.13E+04	-1.38E+07
1.258925	5240.0	5.172E+04	4.717E+00	1.24E-01	1.18E-05	88.3	25.1	28.9	29.0	1.0	1.54E-07	2.93E+03	9.01E+03	-1.23E+07
1.584893	5330.0	5.854E+04	5.713E+00	1.40E-01	1.69E-05	84.3	24.5	27.2	27.4	1.2	1.71E-07	2.60E+03	7.15E+03	-1.08E+07
1.995262	5430.0	6.608E+04	7.041E+00	1.60E-01	2.47E-05	78.9	23.3	25.0	25.3	1.4	1.90E-07	2.28E+03	5.62E+03	-9.26E+06
2.511886	5540.0	7.430E+04	8.868E+00	1.87E-01	3.68E-05	72.0	21.6	22.4	22.8	1.7	2.09E-07	1.91E+03	4.37E+03	-7.77E+06
3.162278	5650.0	8.311E+04	1.128E+01	2.21E-01	5.29E-05	64.6	19.5	19.8	20.2	2.0	2.29E-07	1.55E+03	3.37E+03	-6.31E+06
3.981072	5765.0	9.244E+04	1.457E+01	2.64E-01	7.51E-05	56.7	17.2	17.0	17.5	2.2	2.50E-07	1.31E+03	2.57E+03	-4.89E+06
5.011872	5890.0	1.021E+05	1.926E+01	3.23E-01	1.07E-04	48.4	14.6	14.3	14.7	2.3	2.70E-07	1.17E+03	1.96E+03	-3.54E+06
6.309573	6035.0	1.120E+05	2.650E+01	4.07E-01	1.58E-04	39.6	11.8	11.4	11.7	2.4	2.89E-07	1.06E+03	1.43E+03	-2.26E+06
.7943282	6200.0	1.217E+05	3.786E+01	5.27E-01	2.37E-04	31.0	9.2	8.7	9.0	2.5	3.06E-07	9.67E+02	1.03E+03	-1.08E+06
1.000000	6390.0	1.310E+05	5.644E+01	7.06E-01	3.65E-04	23.2	6.7	6.3	6.5	2.4	3.19E-07	8.87E+02	7.29E+02 C	0.
1.258925	6610.0	1.395E+05	8.796E+01	9.78E-01	5.79E-04	16.6	4.6	4.3	4.4	2.2	3.29E-07	8.08E+02	5.01E+02 C	9.59E+05
1.584893	6860.0	1.472E+05	1.419E+02	1.39E+00	9.40E-04	11.6	3.1	2.8	2.9	2.0	3.34E-07	7.25E+02	3.36E+02 C	1.80E+06
1.995262	7140.0	1.540E+05	2.345E+02	2.02E+00	1.55E-03	7.9	2.0	1.8	1.8	1.7	3.36E-07	6.32E+02	2.20E+02 C	2.53E+06
2.511886	7440.0	1.598E+05	3.872E+02	2.94E+00	2.53E-03	5.4	1.2	1.1	1.2	1.5	3.34E-07	5.29E+02	1.43E+02 C	3.16E+06
3.162277	7750.0	1.648E+05	6.263E+02	4.24E+00	4.04E-03	3.8	.8	.7	.7	1.2	3.30E-07	4.09E+02	9.20E+01 C	3.71E+06
3.981071	8030.0	1.694E+05	9.400E+02	5.83E+00	5.97E-03	2.9	.5	.5	.5	1.1	3.27E-07	2.97E+02	6.21E+01 C	4.21E+06
5.011872	8290.0	1.736E+05	1.340E+03	7.76E+00	8.38E-03	2.2	.4	.3	.4	.9	3.24E-07	2.15E+02	4.31E+01 C	4.68E+06
6.309573	8520.0	1.776E+05	1.805E+03	9.94E+00	1.11E-02	1.8	.3	.3	.3	.8	3.22E-07	1.47E+02	3.12E+01 C	5.14E+06
.7943282	8710.0	1.817E+05	2.288E+03	1.22E+01	1.38E-02	1.6	.2	.2	.2	.7	3.21E-07	9.95E+01	2.38E+01 C	5.60E+06
10.00000	8880.0	1.859E+05	2.810E+03	1.46E+01	1.67E-02	1.4	.2	.2	.2	.7	3.21E-07	7.42E+01	1.87E+01 C	6.08E+06
12.58925	9050.0	1.904E+05	3.427E+03	1.74E+01	1.99E-02	1.2	.2	.1	.2	.6	3.22E-07	5.89E+01	1.47E+01 C	6.58E+06
15.84893	9220.0	1.951E+05	4.152E+03	2.08E+01	2.37E-02	1.1	.1	.1	.1	.6	3.23E-07	4.68E+01	1.15E+01 C	7.11E+06
19.95262	9390.0	2.001E+05	4.999E+03	2.47E+01	2.79E-02	1.0	.1	.1	.1	.5	3.24E-07	3.72E+01	9.11E+00 C	7.67E+06
25.11886	9560.0	2.053E+05	5.983E+03	2.94E+01	3.28E-02	.9	.1	.1	.1	.5	3.25E-07	3.31E+01	7.20E+00 C	8.26E+06

TABLE V

Harvard-Smithsonian reference atmosphere

I EFF = 5780. LOG G = 4.440. HELIUM/HYDROGEN BY NUMBER= .100. ABUNDANCES LW+FE=7.5

OPTICAL DEPTH	TEMP (K)	RAYLEIGH /TOTAL	ELECTRON /TOTAL	OPACITY PER A(H-)	NEUTRAL H A(H)	NEUTRAL H PER GM	CO PER CC	B1	FRACTIONAL IONIZATION OF METALS SI	MG	FE	C	NA	AL
1.00E-08	8930.0	.0014	.9849	3.970E-02	9.197E-01	2.065E+23		1058.000	1.000	1.000	1.000	1.000	1.000	1.000
1.26E-08	8880.0	.0014	.9846	4.064E-02	9.508E-01	2.059E+23		935.000	1.000	1.000	1.000	1.000	1.000	1.000
1.58E-08	8810.0	.0015	.9841	4.156E-02	9.559E-01	2.084E+23		818.000	1.000	1.000	1.000	1.000	1.000	1.000
2.00E-08	8750.0	.0015	.9837	4.262E-02	9.782E-01	2.092E+23		715.000	1.000	1.000	1.000	1.000	1.000	1.000
2.51E-08	8680.0	.0015	.9832	4.365E-02	9.806E-01	2.121E+23		625.000	1.000	1.000	1.000	1.000	1.000	1.000
3.16E-08	8630.0	.0015	.9826	4.535E-02	1.057E+00	2.088E+23		527.000	1.000	1.000	1.000	1.000	1.000	1.000
3.98E-08	8560.0	.0015	.9819	4.676E-02	1.076E+00	2.108E+23		452.000	1.000	1.000	1.000	1.000	1.000	1.000
5.01E-08	8510.0	.0015	.9812	4.862E-02	1.148E+00	2.086E+23		384.000	1.000	1.000	1.000	1.000	1.000	1.000
6.31E-08	8450.0	.0015	.9805	5.051E-02	1.196E+00	2.090E+23		327.000	1.000	1.000	1.000	1.000	1.000	1.000
7.94E-08	8380.0	.0015	.9795	5.304E-02	1.272E+00	2.084E+23		267.000	1.000	1.000	1.000	1.000	1.000	1.000
1.00E-07	8320.0	.0015	.9784	5.579E-02	1.358E+00	2.074E+23		221.000	1.000	1.000	1.000	1.000	1.000	1.000
1.26E-07	8250.0	.0014	.9771	5.924E-02	1.466E+00	2.065E+23		177.000	1.000	1.000	1.000	1.000	1.000	1.000
1.58E-07	8170.0	.0014	.9754	6.355E-02	1.598E+00	2.057E+23		137.000	1.000	1.000	1.000	1.000	1.000	1.000
2.00E-07	8090.0	.0015	.9736	6.758E-02	1.644E+00	2.101E+23		112.000	1.000	1.000	1.000	1.000	1.000	1.000
2.51E-07	8000.0	.0015	.9714	7.289E-02	1.719E+00	2.145E+23		87.800	1.000	1.000	1.000	1.000	1.000	1.000
3.16E-07	7910.0	.0016	.9685	7.992E-02	1.857E+00	2.171E+23		66.300	1.000	1.000	1.000	1.000	1.000	1.000
3.98E-07	7820.0	.0017	.9653	8.745E-02	1.923E+00	2.240E+23		52.000	1.000	1.000	1.000	.999	1.000	1.000
5.01E-07	7710.0	.0019	.9614	9.563E-02	1.870E+00	2.376E+23		41.200	1.000	1.000	1.000	.999	1.000	1.000
6.31E-07	7630.0	.0021	.9569	1.055E-01	1.855E+00	2.496E+23		34.200	1.000	1.000	1.000	.999	1.000	1.000
7.94E-07	7500.0	.0027	.9517	1.144E-01	1.593E+00	2.745E+23		28.800	1.000	1.000	1.000	.999	1.000	1.000
1.00E-06	7360.0	.0036	.9448	1.254E-01	1.342E+00	3.003E+23		23.800	1.000	1.000	1.000	.998	1.000	1.000
1.26E-06	7180.0	.0055	.9369	1.315E-01	9.268E-01	3.349E+23		21.200	1.000	1.000	1.000	.997	1.000	1.000
1.58E-06	6970.0	.0089	.9232	1.415E-01	6.280E-01	3.642E+23		17.200	1.000	1.000	1.000	.994	1.000	1.000
2.00E-06	6720.0	.0158	.8992	1.522E-01	3.825E-01	3.886E+23		13.200	1.000	1.000	1.000	.988	1.000	1.000
2.51E-06	6440.0	.0320	.8494	1.628E-01	1.990E-01	4.060E+23		10.100	1.000	1.000	1.000	.973	1.000	1.000
3.16E-06	6180.0	.0639	.7462	1.826E-01	1.018E-01	4.151E+23		7.800	1.000	1.000	1.000	.934	1.000	1.000
3.98E-06	5950.0	.1054	.5815	2.203E-01	5.936E-02	4.189E+23		5.500	1.000	1.000	1.000	.845	1.000	1.000
5.01E-06	5750.0	.1422	.4026	2.619E-01	3.650E-02	4.206E+23		3.900	.999	1.000	1.000	.692	1.000	1.000
6.31E-06	5590.0	.1606	.2678	3.050E-01	2.509E-02	4.214E+23		2.800	.998	1.000	1.000	.512	1.000	1.000
7.94E-06	5440.0	.1698	.1775	3.375E-01	1.745E-02	4.217E+23		2.000	.997	1.000	.999	.342	1.000	1.000
1.00E-05	5300.0	.1678	.1197	3.774E-01	1.349E-02	4.219E+23	2.242E+06	1.300	.995	1.000	.999	.204	1.000	1.000
1.26E-05	5170.0	.1784	.0801	3.739E-01	8.142E-03	4.221E+23	8.725E+06	1.100	.993	.999	.999	.127	1.000	1.000
1.58E-05	5040.0	.1916	.0531	3.579E-01	4.419E-03	4.222E+23	3.377E+07	1.000	.990	.999	.998	.076	1.000	1.000
2.00E-05	4910.0	.2052	.0348	3.392E-01	2.101E-03	4.223E+23	1.336E+08	1.000	.985	.999	.997	.044	1.000	1.000
2.51E-05	4790.0	.2059	.0235	3.456E-01	1.021E-03	4.223E+23	4.992E+08	1.000	.977	.998	.995	.023	1.000	1.000
3.16E-05	4660.0	.1935	.0162	3.792E-01	4.481E-04	4.223E+23	1.930E+09	1.000	.958	.996	.992	.011	1.000	.999
3.98E-05	4530.0	.1670	.0117	4.574E-01	1.877E-04	4.223E+23	7.094E+09	1.000	.918	.993	.983	.004	1.000	.999
5.01E-05	4400.0	.1378	.0087	5.758E-01	7.445E-05	4.223E+23	2.395E+10	1.000	.836	.985	.965	.002	1.000	.998
6.31E-05	4280.0	.1151	.0066	7.108E-01	3.037E-05	4.223E+23	6.694E+10	1.000	.704	.969	.929	.001	1.000	.996
7.94E-05	4200.0	.1000	.0053	8.376E-01	1.620E-05	4.222E+23	1.313E+11	1.000	.580	.949	.885	.000	1.000	.994
1.00E-04	4170.0	.0890	.0045	9.580E-01	1.272E-05	4.222E+23	1.896E+11	1.000	.510	.934	.853	.000	1.000	.992
1.26E-04	4175.0	.0798	.0039	1.083E+00	1.325E-05	4.222E+23	2.319E+11	1.000	.485	.927	.841	.000	1.000	.991
1.58E-04	4190.0	.0717	.0035	1.220E+00	1.496E-05	4.222E+23	2.712E+11	1.000	.474	.924	.834	.000	1.000	.990
2.00E-04	4205.0	.0645	.0031	1.370E+00	1.686E-05	4.222E+23	3.157E+11	1.000	.463	.920	.828	.000	1.000	.990
2.51E-04	4225.0	.0580	.0028	1.536E+00	1.977E-05	4.221E+23	3.596E+11	1.000	.459	.918	.825	.000	1.000	.989
3.16E-04	4250.0	.0523	.0025	1.719E+00	2.406E-05	4.221E+23	4.011E+11	1.000	.461	.918	.825	.000	1.000	.989
3.98E-04	4280.0	.0471	.0023	1.920E+00	3.037E-05	4.221E+23	4.382E+11	1.000	.469	.920	.829	.000	1.000	.989
5.01E-04	4305.0	.0425	.0021	2.140E+00	3.867E-05	4.221E+23	4.874E+11	1.000	.470	.920	.829	.000	1.000	.988
6.31E-04	4330.0	.0383	.0019	2.392E+00	4.445E-05	4.221E+23	5.418E+11	1.000	.472	.920	.829	.000	1.000	.988
7.94E-04	4355.0	.0345	.0017	2.666E+00	5.360E-05	4.221E+23	6.016E+11	1.000	.473	.920	.829	.000	1.000	.988

I EFF = 5780. LOG G = 4.440. HELIUM/HYDROGEN BY NUMBER= .100. ABUNDANCES LW+FE=7.5

OPTICAL DEPTH	TEMP (K)	RAYLEIGH /TOTAL	ELECTRON /TOTAL	OPACITY PER A(H-)	NEUTRAL H A(H)	NEUTRAL H PER GM	CO PER CC	B1	FRACTIONAL IONIZATION OF METALS SI	MG	FE	C	NA	AL
.0010000	4380.0	.0312	.0015	2.969E+00	6.450E-05	4.221E+23	6.680E+11	1.000	.474	.919	.830	.000	1.000	.987
.0012589	4405.0	.0281	.0014	3.306E+00	7.745E-05	4.220E+23	7.416E+11	1.000	.475	.919	.830	.000	1.000	.987
.0015849	4430.0	.0254	.0012	3.680E+00	9.282E-05	4.220E+23	8.233E+11	1.000	.476	.919	.829	.000	.999	.987
.0019953	4460.0	.0229	.0011	4.093E+00	1.150E-04	4.220E+23	8.961E+11	1.000	.482	.920	.832	.000	.999	.987
.0025119	4490.0	.0207	.0010	4.550E+00	1.421E-04	4.220E+23	9.754E+11	1.000	.488	.921	.835	.000	.999	.986
.0031623	4525.0	.0186	.0009	5.057E+00	1.813E-04	4.220E+23	1.040E+12	1.000	.499	.923	.840	.000	.999	.986
.0039811	4550.0	.0168	.0008	5.621E+00	2.152E-04	4.220E+23	1.156E+12	1.000	.498	.923	.839	.000	.999	.986
.0050119	4575.0	.0152	.0008	6.247E+00	2.550E-04	4.219E+23	1.285E+12	1.000	.498	.922	.838	.000	.999	.985
.0063096	4600.0	.0137	.0007	6.942E+00	3.017E-04	4.219E+23	1.429E+12	1.000	.497	.921	.837	.000	.999	.985
.0079433	4630.0	.0124	.0006	7.711E+00	3.681E-04	4.219E+23	1.559E+12	1.000	.501	.922	.839	.000	.999	.985
.0100000	4660.0	.0112	.0006	8.564E+00	4.481E-04	4.219E+23	1.701E+12	1.000	.505	.922	.840	.000	.999	.984
.0125893	4690.0	.0101	.0005	9.511E+00	5.440E-04	4.219E+23	1.858E+12	1.000	.508	.923	.841	.001	.999	.984
.0158489	4720.0	.0091	.0005	1.056E+01	6.589E-04	4.218E+23	2.031E+12	1.000	.511	.923	.842	.001	.999	.984
.0199526	4750.0	.0082	.0004	1.173E+01	7.962E-04	4.218E+23	2.221E+12	1.000	.514	.923	.843	.001	.999	.983
.0251189	4790.0	.0074	.0004	1.302E+01	1.021E-03	4.218E+23	2.331E+12	1.000	.525	.926	.849	.001	.999	.983
.0316228	4840.0	.0067	.0004	1.445E+01	1.385E-03	4.218E+23	2.347E+12	1.000	.546	.930	.858	.001	.999	.984
.0398107	4895.0	.0060	.0003	1.604E+01	1.924E-03	4.218E+23	2.313E+12	1.000	.569	.935	.868	.001	.999	.984
.0501187	4950.0	.0054	.0003	1.781E+01	2.652E-03	4.218E+23	2.278E+12	1.000	.591	.940	.878	.001	.999	.985
.0630957	5010.0	.0049	.0003	1.979E+01	3.735E-03	4.218E+23	2.194E+12	1.000	.616	.945	.887	.001	.999	.986
.0794328	5080.0	.0044	.0003	2.202E+01	5.513E-03	4.218E+23	2.021E+12	1.000	.646	.950	.899	.002	.999	.986
.1000000	5160.0	.0039	.0002	2.458E+01	8.493E-03	4.218E+23	1.780E+12	1.000	.680	.956	.911	.002	.999	.987
.1258925	5240.0	.0035	.0002	2.756E+01	1.291E-02	4.218E+23	1.570E+12	1.000	.710	.961	.921	.003	.999	.988
.1584893	5330.0	.0031	.0002	3.113E+01	2.039E-02	4.219E+23	1.325E+12	1.000	.741	.966	.931	.004	.999	.989
.1995262	5430.0	.0027	.0002	3.559E+01	3.327E-02	4.219E+23	1.072E+12	1.000	.771	.971	.940	.005	.999	.990
.2511886	5540.0	.0023	.0002	4.136E+01	5.588E-02	4.219E+23	8.317E+11	1.000	.799	.974	.948	.006	.999	.991
.3162278	5650.0	.0020	.0002	4.864E+01	9.198E-02	4.220E+23	6.477E+11	1.000	.821	.977	.954	.008	.999	.991
.3981072	5765.0	.0016	.0002	5.803E+01	1.518E-01	4.220E+23	4.953E+11	1.000	.839	.979	.959	.011	.999	.991
.5011872	5890.0	.0013	.0002	7.055E+01	2.560E-01	4.220E+23	3.651E+11	1.000	.855	.981	.963	.014	.999	.992
.6309573	6035.0	.0011	.0002	8.833E+01	4.570E-01	4.220E+23	2.500E+11	1.000	.870	.983	.967	.018	.999	.992
.7943282	6200.0	.0008	.0002	1.138E+02	8.552E-01	4.220E+23	1.602E+11	1.000	.884	.985	.971	.024	.999	.992
1.000000	6390.0	.0006	.0002	1.513E+02	1.691E+00	4.220E+23	9.519E+10	1.000	.896	.986	.974	.032	.999	.992
1.258925	6610.0	.0004	.0002	2.078E+02	3.549E+00	4.219E+23	5.218E+10	1.000	.908	.988	.977	.043	.999	.992
1.584893	6860.0	.0003	.0002	2.924E+02	7.782E+00	4.218E+23	2.680E+10	1.000	.919	.989	.979	.060	.999	.992
1.995262	7140.0	.0002	.0002	4.180E+02	1.758E+01	4.216E+23	1.309E+10	1.000	.929	.990	.981	.082	.999	.992
2.511886	7440.0	.0001	.0003	5.957E+02	3.935E+01	4.212E+23	6.341E+09	1.000	.937	.991	.983	.112	.999	.992
3.162277	7750.0	.0001	.0003	8.347E+02	8.480E+01	4.206E+23		1.000	.944	.992	.985	.148	.999	.992
3.981071	8030.0	.0001	.0003	1.108E+03	1.613E+02	4.198E+23		1.000	.950	.992	.986	.185	.999	.992
5.011872	8290.0	.0001	.0003	1.416E+03	2.821E+02	4.188E+23		1.000	.954	.993	.988	.223	.999	.992
6.309573	8520.0	.0000	.0003	1.739E+03	4.496E+02	4.176E+23		1.000	.957	.993	.988	.259	.999	.992
7.943282	8710.0	.0000	.0003	2.047E+03	6.488E+02	4.165E+23		1.000	.960	.994	.989	.290	.999	.992
10.00000	8880.0	.0000	.0003	2.357E+03	8.890E+02	4.153E+23		1.000	.962	.994	.989	.317	.999	.992
12.58925	9050.0	.0000	.0003	2.700E+03	1.204E+03	4.139E+23		1.000	.963	.994	.990	.345	.999	.992
15.84893	9220.0	.0000	.0003	3.077E+03	1.613E+03	4.123E+23		1.000	.965	.994	.990	.372	.999	.992
19.95262	9390.0	.0000	.0003	3.491E+03	2.138E+03	4.105E+23		1.000	.967	.994	.991	.400	.999	.992
25.11886	9560.0	.0000	.0003	3.942E+03	2.805E+03	4.085E+23		1.000	.968	.995	.991	.427	.999	.992

TABLE VI

SPECIFIC INTENSITY AND PHI FOR LIMB DARKENING — HARVARD SMITHSONIAN REFERENCE ATMOSPHERE

MU	910.0-	910.0+	912.0+	912.0+	1000.0	1000.0	1099.0-	1100.0+	1100.0+
1.000	1.2541E-11	4.5400E+09	3.4187E-13	1.2322E+08	2.9834E-12	8.9439E+08	2.2084E-11	5.4816E+09	2.7335E-12	6.7724E+08
.800	1.2308E-11	9.8147E-01	4.1173E-13	1.2044E+00	3.5171E-12	1.1789E+00	2.5552E-11	1.1570E+00	3.3544E-12	1.2272E+00
.600	1.1667E-11	9.3036E-01	4.8882E-13	1.4299E+00	4.1437E-12	1.3889E+00	2.9893E-11	1.3536E+00	4.3491E-12	1.5911E+00
.500	1.1618E-11	9.2667E-01	5.4781E-13	1.6024E+00	4.6248E-12	1.5502E+00	3.3130E-11	1.5002E+00	4.9829E-12	1.8229E+00
.400	1.1281E-11	8.9959E-01	6.4931E-13	1.8993E+00	5.3961E-12	1.8087E+00	3.8070E-11	1.7238E+00	6.0597E-12	2.2169E+00
.300	1.0976E-11	8.7520E-01	7.7467E-13	2.2660E+00	6.3403E-12	2.1252E+00	4.4207E-11	2.0017E+00	7.6697E-12	2.8059E+00
.250	1.0743E-11	8.5663E-01	8.6442E-13	2.5285E+00	7.0168E-12	2.3520E+00	4.8466E-11	2.1946E+00	8.7602E-12	3.2048E+00
.200	1.0634E-11	8.4797E-01	9.9355E-13	2.9063E+00	8.0108E-12	2.6852E+00	5.4773E-11	2.4802E+00	1.0463E-11	3.8279E+00
.150	1.0438E-11	8.3230E-01	1.2271E-12	3.5895E+00	9.6355E-12	3.2297E+00	6.4467E-11	2.9191E+00	1.2984E-11	4.7499E+00
.100	1.0269E-11	8.1883E-01	1.5252E-12	4.4613E+00	1.1832E-11	3.9658E+00	7.8037E-11	3.5336E+00	1.7061E-11	6.2417E+00

SPECIFIC INTENSITY AND PHI FOR LIMB DARKENING — HARVARD SMITHSONIAN REFERENCE ATMOSPHERE

MU	1196.0-	1196.0+	1198.0+	1198.0+	1238.0-	1238.0-	1239.0+	1239.0+	1350.0	1350.0
1.000	1.6244E-11	3.4045E+09	9.3989E-12	1.9633E+09	1.7569E-11	3.4365E+09	1.2121E-12	2.3671E+08	9.1810E-12	1.5102E+09
.800	1.9735E-11	1.2149E+00	1.1739E-11	1.2490E+00	2.1876E-11	1.2451E+00	1.5095E-12	1.2454E+00	1.1148E-11	1.2142E+00
.600	2.4893E-11	1.5324E+00	1.5352E-11	1.6334E+00	2.8470E-11	1.6205E+00	2.0114E-12	1.6594E+00	1.4309E-11	1.5586E+00
.500	2.8506E-11	1.7549E+00	1.8336E-11	1.9509E+00	3.3874E-11	1.9281E+00	2.3991E-12	1.9793E+00	1.6749E-11	1.8243E+00
.400	3.4106E-11	2.0996E+00	2.2043E-11	2.3453E+00	4.0698E-11	2.3165E+00	3.0023E-12	2.4770E+00	2.0322E-11	2.2135E+00
.300	4.2268E-11	2.6020E+00	2.8416E-11	3.0233E+00	5.2134E-11	2.9674E+00	4.0062E-12	3.3052E+00	2.6010E-11	2.8331E+00
.250	4.7920E-11	2.9500E+00	3.3240E-11	3.5366E+00	6.0794E-11	3.4603E+00	4.8033E-12	3.9628E+00	3.0390E-11	3.3101E+00
.200	5.6142E-11	3.4561E+00	3.9675E-11	4.2213E+00	7.2402E-11	4.1210E+00	5.9740E-12	4.9286E+00	3.6594E-11	3.9858E+00
.150	6.8495E-11	4.2166E+00	4.9980E-11	5.3176E+00	9.0637E-11	5.1589E+00	7.8682E-12	6.4914E+00	4.6453E-11	5.0597E+00
.100	8.7959E-11	5.4148E+00	6.7270E-11	7.1572E+00	1.2147E-10	6.9141E+00	1.1524E-11	9.5073E+00	6.4450E-11	7.0199E+00

SPECIFIC INTENSITY AND PHI FOR LIMB DARKENING — HARVARD SMITHSONIAN REFERENCE ATMOSPHERE

MU	1443.0-	1443.0+	1444.0+	1444.0+	1527.2-	1527.2+	1527.2+	1527.2+	1600.0	1600.0
1.000	3.2019E-11	4.6098E+09	3.0851E-11	4.4357E+09	8.3547E-11	1.0739E+10	3.4912E-11	4.4875E+09	9.0275E-11	1.0572E+10
.800	3.8357E-11	1.1980E+00	3.6743E-11	1.1910E+00	9.8444E-11	1.1783E+00	3.3394E-11	9.5651E-01	8.3824E-11	9.2854E-01
.600	4.8443E-11	1.5130E+00	4.5998E-11	1.4909E+00	1.2174E-10	1.4572E+00	3.3265E-11	9.5281E-01	8.0103E-11	8.8732E-01
.500	5.5975E-11	1.7482E+00	5.3137E-11	1.7224E+00	1.3957E-10	1.6706E+00	3.4183E-11	9.7911E-01	8.0114E-11	8.8744E-01
.400	6.7040E-11	2.0938E+00	6.3136E-11	2.0465E+00	1.6422E-10	1.9656E+00	3.6412E-11	1.0429E+00	8.2499E-11	9.1386E-01
.300	8.4537E-11	2.6402E+00	7.8899E-11	2.5574E+00	2.0279E-10	2.4272E+00	4.1553E-11	1.1902E+00	9.0040E-11	9.9739E-01
.250	9.7464E-11	3.0440E+00	9.0903E-11	2.9465E+00	2.3170E-10	2.7733E+00	4.6151E-11	1.3219E+00	9.7876E-11	1.0842E+00
.200	1.1611E-10	3.6263E+00	1.0746E-10	3.4831E+00	2.7157E-10	3.2505E+00	5.3529E-11	1.5332E+00	1.1069E-10	1.2261E+00
.150	1.4524E-10	4.5362E+00	1.3328E-10	4.3201E+00	3.3309E-10	3.9869E+00	6.6177E-11	1.8955E+00	1.3311E-10	1.4745E+00
.100	1.9710E-10	6.1558E+00	1.7945E-10	5.8164E+00	4.4130E-10	5.2820E+00	9.1725E-11	2.6273E+00	1.7883E-10	1.9809E+00

SPECIFIC INTENSITY AND PHI FOR LIMB DARKENING — HARVARD SMITHSONIAN REFERENCE ATMOSPHERE

MU	1683.3-	1683.3+	1683.3+	1683.3+	1699.9-	1699.9-	1700.1+	1700.1+	1800.0	1800.0
1.000	2.0722E-10	2.1925E+10	1.5204E-09	1.6087E+11	2.0387E-09	2.1151E+11	1.4227E-08	1.4756E+12	5.7225E-08	5.2949E+12
.800	1.9570E-10	9.4444E-01	1.0962E-09	7.2097E-01	1.3517E-09	6.6299E-01	7.1291E-09	5.0111E-01	2.5227E-08	4.4083E-01
.600	1.8994E-10	9.1662E-01	7.8202E-10	5.1435E-01	9.2867E-10	4.5552E-01	3.6358E-09	2.5557E-01	1.0395E-08	1.8165E-01
.500	1.9108E-10	9.2212E-01	6.5709E-10	4.3218E-01	7.7290E-10	3.7911E-01	2.5996E-09	1.8273E-01	6.7520E-09	1.1799E-01
.400	1.9797E-10	9.5539E-01	5.4267E-10	3.5692E-01	6.3490E-10	3.1142E-01	1.8391E-09	1.2927E-01	4.4282E-09	7.7382E-02
.300	2.1667E-10	1.0456E+00	4.3601E-10	2.8678E-01	5.0842E-10	2.4938E-01	1.2828E-09	9.0167E-02	2.9641E-09	5.1796E-02
.250	2.3504E-10	1.1343E+00	3.8577E-10	2.5373E-01	4.4939E-10	2.2043E-01	1.0547E-09	7.4135E-02	2.4162E-09	4.2222E-02
.200	2.6417E-10	1.2748E+00	3.3542E-10	2.2061E-01	3.9053E-10	1.9156E-01	8.5693E-10	6.0235E-02	1.9586E-09	3.4227E-02
.150	3.1477E-10	1.5190E+00	2.8659E-10	1.8850E-01	3.3328E-10	1.6348E-01	6.8170E-10	4.7918E-02	1.5617E-09	2.7290E-02
.100	4.1492E-10	2.0023E+00	2.4509E-10	1.6120E-01	2.8435E-10	1.3947E-01	5.2163E-10	3.6666E-02	1.1973E-09	2.0923E-02

SPECIFIC INTENSITY AND PHI FOR LIMB DARKENING — HARVARD SMITHSONIAN REFERENCE ATMOSPHERE

MU	5500.0	5500.0	6000.0	6000.0	7000.0	7000.0	8000.0	8000.0	10000.0	10000.0
1.000	3.6686E-05	3.6357E+14	3.8635E-05	3.2174E+14	4.0816E-05	2.4972E+14	4.1430E-05	1.9407E+14	4.0607E-05	1.2174E+14
.800	3.2578E-05	8.8802E-01	3.4685E-05	8.9776E-01	3.7267E-05	9.1304E-01	3.8277E-05	9.2390E-01	3.7988E-05	9.3550E-01
.600	2.8127E-05	7.6669E-01	3.0383E-05	7.8640E-01	3.3356E-05	8.1722E-01	3.4762E-05	8.3905E-01	3.5038E-05	8.6285E-01
.500	2.5747E-05	7.0181E-01	2.8066E-05	7.2643E-01	3.1214E-05	7.6474E-01	3.2816E-05	7.9207E-01	3.3388E-05	8.2223E-01
.400	2.3236E-05	6.3337E-01	2.5598E-05	6.6255E-01	2.8902E-05	7.0811E-01	3.0692E-05	7.4082E-01	3.1576E-05	7.7760E-01
.300	2.0535E-05	5.5975E-01	2.2906E-05	5.9288E-01	2.6343E-05	6.4541E-01	2.8315E-05	6.8344E-01	2.9525E-05	7.2710E-01
.250	1.9077E-05	5.2001E-01	2.1442E-05	5.5499E-01	2.4922E-05	6.1061E-01	2.6981E-05	6.5123E-01	2.8365E-05	6.9853E-01
.200	1.7511E-05	4.7733E-01	1.9853E-05	5.1386E-01	2.3366E-05	5.7248E-01	2.5508E-05	6.1567E-01	2.7074E-05	6.6674E-01
.150	1.5783E-05	4.3023E-01	1.8080E-05	4.6798E-01	2.1607E-05	5.2939E-01	2.3828E-05	5.7513E-01	2.5589E-05	6.3017E-01
.100	1.3791E-05	3.7591E-01	1.6017E-05	4.1456E-01	1.9522E-05	4.7829E-01	2.1817E-05	5.2660E-01	2.3787E-05	5.8579E-01

SPECIFIC INTENSITY AND PHI FOR LIMB DARKENING — HARVARD SMITHSONIAN REFERENCE ATMOSPHERE

MU	14000.0	14000.0	16500.0	16500.0	25000.0	25000.0	50000.0	50000.0	100000.0	100000.0
1.000	3.6678E-05	5.6101E+13	3.3373E-05	3.6749E+13	1.6735E-05	8.0271E+12	4.6883E-06	5.6220E+11	1.2206E-06	3.6593E+10
.800	3.4862E-05	9.5049E-01	3.2022E-05	9.5952E-01	1.6201E-05	9.6809E-01	4.5957E-06	9.8025E-01	1.2045E-06	9.8678E-01
.600	3.2698E-05	8.9147E-01	3.0368E-05	9.0996E-01	1.5563E-05	9.2996E-01	4.4847E-06	9.5657E-01	1.1852E-06	9.7099E-01
.500	3.1439E-05	8.5717E-01	2.9380E-05	8.8035E-01	1.5188E-05	9.0760E-01	4.4187E-06	9.4251E-01	1.1738E-06	9.6164E-01
.400	3.0016E-05	8.1836E-01	2.8237E-05	8.4611E-01	1.4761E-05	8.8203E-01	4.3422E-06	9.2617E-01	1.1607E-06	9.5095E-01
.300	2.8362E-05	7.7328E-01	2.6879E-05	8.0540E-01	1.4253E-05	8.5171E-01	4.2503E-06	9.0658E-01	1.1452E-06	9.3823E-01
.250	2.7412E-05	7.4736E-01	2.6084E-05	7.8160E-01	1.3955E-05	8.3387E-01	4.1957E-06	8.9494E-01	1.1361E-06	9.3077E-01
.200	2.6341E-05	7.1817E-01	2.5175E-05	7.5436E-01	1.3612E-05	8.1341E-01	4.1327E-06	8.8150E-01	1.1257E-06	9.2223E-01
.150	2.5092E-05	6.8411E-01	2.4103E-05	7.2223E-01	1.3203E-05	7.8895E-01	4.0574E-06	8.6543E-01	1.1133E-06	9.1205E-01
.100	2.3548E-05	6.4203E-01	2.2759E-05	6.8196E-01	1.2678E-05	7.5760E-01	3.9619E-06	8.4508E-01	1.0975E-06	8.9918E-01

SPECIFIC INTENSITY AND PHI FOR LIMB DARKENING — HARVARD SMITHSONIAN REFERENCE ATMOSPHERE

MU	200000.0	200000.0	500000.0	500000.0	100.0	100.0	200.0	200.0	300.0	300.0
1.000	3.0706E-07	2.3013E+09	4.8687E-08	5.8383E-07	1.2022E-08	3.6041E+06	3.0026E-09	2.2504E+05	1.3642E-09	4.5442E+04
.800	3.0444E-07	9.9145E-01	4.8442E-08	9.9499E-01	1.1980E-08	9.9648E-01	3.0105E-09	1.0026E+00	1.3780E-09	1.0101E+00
.600	3.0131E-07	9.8126E-01	4.8135E-08	9.8868E-01	1.1934E-08	9.9268E-01	3.0284E-09	1.0086E+00	1.4015E-09	1.0273E+00
.500	2.9946E-07	9.7526E-01	4.7944E-08	9.8475E-01	1.1913E-08	9.9092E-01	3.0448E-09	1.0140E+00	1.4199E-09	1.0409E+00
.400	2.9735E-07	9.6837E-01	4.7721E-08	9.8017E-01	1.1895E-08	9.8945E-01	3.0711E-09	1.0228E+00	1.4465E-09	1.0604E+00
.300	2.9480E-07	9.6007E-01	4.7456E-08	9.7473E-01	1.1891E-08	9.8911E-01	3.1168E-09	1.0380E+00	1.4871E-09	1.0901E+00
.250	2.9327E-07	9.5507E-01	4.7300E-08	9.7151E-01	1.1901E-08	9.8995E-01	3.1533E-09	1.0502E+00	1.5163E-09	1.1115E+00
.200	2.9152E-07	9.4940E-01	4.7129E-08	9.6800E-01	1.1930E-08	9.9235E-01	3.2068E-09	1.0680E+00	1.5555E-09	1.1402E+00
.150	2.8947E-07	9.4270E-01	4.6943E-08	9.6419E-01	1.1998E-08	9.9800E-01	3.2899E-09	1.0957E+00	1.6102E-09	1.1803E+00
.100	2.8674E-07	9.3383E-01	4.6780E-08	9.6083E-01	1.2162E-08	1.0117E+00	3.4327E-09	1.1432E+00	1.6924E-09	1.2406E+00

SPECIFIC INTENSITY AND PHI FOR LIMB DARKENING — HARVARD SMITHSONIAN REFERENCE ATMOSPHERE

MU	500.0	500.0	1000.0	1000.0	2000.0	2000.0	5000.0	5000.0	10000.0	10000.0
1.000	5.2863E-10	6.3391E+03	1.5716E-10	4.7116E+02	4.6743E-11	3.5034E+01	8.6641E-12	1.0390E+00	2.2854E-12	6.8513E-02
.800	5.4074E-10	1.0229E+00	1.6162E-10	1.0284E+00	4.7823E-11	1.0231E+00	8.7484E-12	1.0097E+00	2.3002E-12	1.0065E+00
.600	5.5856E-10	1.0566E+00	1.6739E-10	1.0651E+00	4.9149E-11	1.0514E+00	8.8488E-12	1.0213E+00	2.3181E-12	1.0143E+00
.500	5.7088E-10	1.0799E+00	1.7106E-10	1.0884E+00	4.9940E-11	1.0683E+00	8.9081E-12	1.0282E+00	2.3288E-12	1.0190E+00
.400	5.8684E-10	1.1101E+00	1.7554E-10	1.1169E+00	5.0845E-11	1.0877E+00	8.9771E-12	1.0361E+00	2.3412E-12	1.0244E+00
.300	6.0820E-10	1.1505E+00	1.8130E-10	1.1536E+00	5.1901E-11	1.1103E+00	9.0625E-12	1.0460E+00	2.3563E-12	1.0310E+00
.250	6.2214E-10	1.1769E+00	1.8491E-10	1.1766E+00	5.2503E-11	1.1232E+00	9.1131E-12	1.0518E+00	2.3652E-12	1.0349E+00
.200	6.3953E-10	1.2098E+00	1.8925E-10	1.2042E+00	5.3180E-11	1.1377E+00	9.1736E-12	1.0588E+00	2.3756E-12	1.0395E+00
.150	6.6204E-10	1.2524E+00	1.9464E-10	1.2384E+00	5.3956E-11	1.1543E+00	9.2469E-12	1.0673E+00	2.3880E-12	1.0449E+00
.100	6.9397E-10	1.3128E+00	2.0162E-10	1.2829E+00	5.4907E-11	1.1746E+00	9.3420E-12	1.0782E+00	2.4036E-12	1.0517E+00

Table VI (continued)

SPECIFIC INTENSITY AND PHI FOR LIMB DARKENING HARVARD SMITHSONIAN REFERENCE ATMOSPHERE

MU	1950.0	1950.0	2077.5-	2077.5-	2077.6+	2077.6+	2300.0	2300.0	2516.0-	2516.0-
1.000	1.9079E-07	1.5042E+13	6.9791E-07	4.8477E+13	2.3715E-06	1.6471E+14	3.4980E-06	1.9823E+14	3.0630E-06	1.4506E+14
.800	8.7221E-08	4.5715E-01	4.0356E-07	5.7822E-01	1.7409E-06	7.3410E-01	2.5982E-06	7.4277E-01	2.1648E-06	7.0675E-01
.600	3.6102E-08	1.8922E-01	1.8335E-07	2.6272E-01	1.1298E-06	4.7640E-01	1.7270E-06	4.9373E-01	1.3489E-06	4.4038E-01
.500	2.3019E-08	1.2065E-01	1.1185E-07	1.6032E-01	8.4825E-07	3.5768E-01	1.3144E-06	3.7577E-01	9.9863E-07	3.2603E-01
.400	1.4873E-08	7.7954E-02	6.4956E-08	9.3073E-02	5.8781E-07	2.4787E-01	9.3577E-07	2.6752E-01	6.9721E-07	2.2762E-01
.300	9.7226E-09	5.0959E-02	3.6867E-08	5.2826E-02	3.6650E-07	1.5455E-01	6.0283E-07	1.7234E-01	4.5572E-07	1.4878E-01
.250	7.9250E-09	4.1537E-02	2.7623E-08	3.9579E-02	2.7309E-07	1.1516E-01	4.6041E-07	1.3162E-01	3.5794E-07	1.1686E-01
.200	6.4034E-09	3.3562E-02	2.0616E-08	2.9539E-02	1.9370E-07	8.1680E-02	3.3562E-07	9.5946E-02	2.7410E-07	8.9487E-02
.150	5.1272E-09	2.6873E-02	1.5417E-08	2.2091E-02	1.2783E-07	5.3901E-02	2.2932E-07	6.5558E-02	2.0398E-07	6.6595E-02
.100	3.9426E-09	2.0664E-02	1.1328E-08	1.6231E-02	7.5218E-08	3.1718E-02	1.4117E-07	4.0357E-02	1.4507E-07	4.7361E-02

SPECIFIC INTENSITY AND PHI FOR LIMB DARKENING HARVARD SMITHSONIAN REFERENCE ATMOSPHERE

MU	2518.0+	2518.0+	2665.0	2665.0	2885.0	2885.0	3000.0	3000.0	3200.0	3200.0
1.000	6.4388E-06	3.0445E+14	7.7882E-06	3.2874E+14	9.9627E-06	3.5884E+14	1.1059E-05	3.6837E+14	1.2950E-05	3.7914E+14
.800	5.1275E-06	7.9634E-01	6.2772E-06	8.0599E-01	8.1699E-06	8.2005E-01	9.1434E-06	8.2680E-01	1.0844E-05	8.3732E-01
.600	3.7718E-06	5.8580E-01	4.7091E-06	6.0464E-01	6.2866E-06	6.3101E-01	7.1114E-06	6.4306E-01	8.5901E-06	6.6331E-01
.500	3.0864E-06	4.7935E-01	3.9048E-06	5.0138E-01	5.3157E-06	5.3356E-01	6.0645E-06	5.4839E-01	7.4148E-06	5.7256E-01
.400	2.4098E-06	3.7426E-01	3.1075E-06	3.9900E-01	4.3321E-06	4.3483E-01	4.9864E-06	4.5181E-01	6.2127E-06	4.7973E-01
.300	1.7561E-06	2.7273E-01	2.3244E-06	2.9845E-01	3.3475E-06	3.3600E-01	3.9159E-06	3.5410E-01	4.9752E-06	3.8418E-01
.250	1.4431E-06	2.2412E-01	1.9434E-06	2.4954E-01	2.8575E-06	2.8682E-01	3.3722E-06	3.0494E-01	4.3429E-06	3.3535E-01
.200	1.1435E-06	1.7760E-01	1.5718E-06	2.0182E-01	2.3689E-06	2.3777E-01	2.8263E-06	2.5557E-01	3.6980E-06	2.8555E-01
.150	8.5828E-07	1.3330E-01	1.2108E-06	1.5546E-01	1.8802E-06	1.8872E-01	2.2728E-06	2.0552E-01	3.0333E-06	2.3422E-01
.100	5.8803E-07	9.1326E-02	8.5755E-07	1.1011E-01	1.3838E-06	1.3890E-01	1.7026E-06	1.5396E-01	2.3321E-06	1.8008E-01

SPECIFIC INTENSITY AND PHI FOR LIMB DARKENING HARVARD SMITHSONIAN REFERENCE ATMOSPHERE

MU	3400.0	3400.0	3647.1-	3647.1-	3647.1+	3647.1+	3800.0	3800.0	4000.0	4000.0
1.000	1.4802E-05	3.8388E+14	1.7014E-05	3.8347E+14	2.1691E-05	4.8889E+14	2.3154E-05	4.8071E+14	2.5882E-05	4.8494E+14
.800	1.2524E-05	8.4609E-01	1.4575E-05	8.5669E-01	1.7957E-05	8.2787E-01	1.9307E-05	8.3382E-01	2.1824E-05	8.4322E-01
.600	1.0090E-05	6.8162E-01	1.1954E-05	7.0261E-01	1.4083E-05	6.4927E-01	1.5308E-05	6.6114E-01	1.7569E-05	6.7882E-01
.500	8.8076E-06	5.9501E-01	1.0566E-05	6.2105E-01	1.2101E-05	5.5786E-01	1.3258E-05	5.7260E-01	1.5366E-05	5.9371E-01
.400	7.4808E-06	5.0538E-01	9.1094E-06	5.3541E-01	1.0122E-05	4.6664E-01	1.1202E-05	4.8380E-01	1.3135E-05	5.0748E-01
.300	6.1033E-06	4.1232E-01	7.5737E-06	4.4515E-01	8.1511E-06	3.7578E-01	9.1401E-06	3.9475E-01	1.0866E-05	4.1985E-01
.250	5.3898E-06	3.6412E-01	6.7654E-06	3.9764E-01	7.1687E-06	3.3049E-01	8.0990E-06	3.4978E-01	9.7068E-06	3.7504E-01
.200	4.6519E-06	3.1427E-01	5.9208E-06	3.4800E-01	6.1804E-06	2.8493E-01	7.0441E-06	3.0422E-01	8.5195E-06	3.2917E-01
.150	3.8795E-06	2.6208E-01	5.0219E-06	2.9517E-01	5.1718E-06	2.3843E-01	5.9574E-06	2.5729E-01	7.2814E-06	2.8133E-01
.100	3.0473E-06	2.0587E-01	4.0346E-06	2.3714E-01	4.1056E-06	1.8928E-01	4.7921E-06	2.0696E-01	5.9360E-06	2.2935E-01

SPECIFIC INTENSITY AND PHI FOR LIMB DARKENING HARVARD SMITHSONIAN REFERENCE ATMOSPHERE

MU	4200.0	4200.0	4400.0	4400.0	4600.0	4600.0	4800.0	4800.0	5000.0	5000.0
1.000	2.7791E-05	4.7231E+14	2.9515E-05	4.5704E+14	3.1068E-05	4.4016E+14	3.2457E-05	4.2232E+14	3.4001E-05	4.0772E+14
.800	2.3647E-05	8.5087E-01	2.5324E-05	8.5800E-01	2.6860E-05	8.6455E-01	2.8255E-05	8.7053E-01	2.9789E-05	8.7614E-01
.600	1.9279E-05	6.9369E-01	2.0875E-05	7.0727E-01	2.2359E-05	7.1968E-01	2.3737E-05	7.3134E-01	2.5245E-05	7.4249E-01
.500	1.7004E-05	6.1185E-01	1.8554E-05	6.2865E-01	2.0010E-05	6.4408E-01	2.1369E-05	6.5838E-01	2.2848E-05	6.7198E-01
.400	1.4684E-05	5.2836E-01	1.6168E-05	5.4779E-01	1.7576E-05	5.6573E-01	1.8906E-05	5.8248E-01	2.0341E-05	5.9826E-01
.300	1.2302E-05	4.4265E-01	1.3692E-05	4.6392E-01	1.5031E-05	4.8383E-01	1.6314E-05	5.0265E-01	1.7689E-05	5.2027E-01
.250	1.1073E-05	3.9844E-01	1.2405E-05	4.2041E-01	1.3701E-05	4.4100E-01	1.4944E-05	4.6043E-01	1.6275E-05	4.7867E-01
.200	9.8024E-06	3.5271E-01	1.1068E-05	3.7500E-01	1.2303E-05	3.9601E-01	1.3499E-05	4.1590E-01	1.4776E-05	4.3457E-01
.150	8.4613E-06	3.0446E-01	9.6383E-06	3.2656E-01	1.0799E-05	3.4761E-01	1.1936E-05	3.6775E-01	1.3145E-05	3.8661E-01
.100	6.9892E-06	2.5149E-01	8.0540E-06	2.7288E-01	9.1176E-06	2.9348E-01	1.0169E-05	3.1332E-01	1.1288E-05	3.3198E-01

shown in Table II. The adopted iron abundance reflects the higher determination by Garz *et al.* (1969); however, the model is relatively little affected by this choice. Oxygen is included in order to calculate N_{CO}, and sulfur is included because of its ultraviolet absorption edge.

The number density of CO has been calculated from the equation

$$N_{CO} = N_C \cdot N_O / [214\, T^{1/2} (e^{49.57 - 128800/T})\,(1 - e^{3100/T})],$$

which uses the simple harmonic oscillator and rigid rotator approximations in the CO partition function. The formation of CO locks up a substantial proportion of the neutral C and O, and these abundances were iterated accordingly. No attempt was made in the same calculation to allow for the ionization of C or O, and therefore the N_{CO} column in Table V is inaccurate where C is ionized. Since the carbon absorption edges are formed in layers where CO is insignificant, the depletion of neutral carbon by the formation of CO was not considered in the carbon-opacity calculations.

The sources of opacity used in establishing the monochromatic opacity at 5000 Å (Table IV) were neutral H, H^-, H_2^+, an analytic hydrogenic summation of high levels of Si and Mg, and Rayleigh and electron scattering. Electron scattering predominates nearly to $\tau_{5000} = 10^{-5}$, and soon thereafter H^- contributes over 90% of the opacity.

TABLE VII

Monochromatic optical depths at selected wavelengths, Harvard-Smithsonian reference atmosphere

TAU	910.0-	912.0+	1000.0	1099.0-	1100.0+	1196.0-	1198.0+	1238.0-	1239.0+	1350.0	1443.0-	1444.0+	1527.2-
1.00E-08	.0000	.0000	.0000	.0000	.0000	.0000	.0000	.0000	.0000	.0000	.0000	.0000	.0000
3.16E-08	.1945	.0000	.0000	.0000	.0000	.0000	.0000	.0000	.0000	.0000	.0000	.0000	.0000
1.00E-07	.8046	.0000	.0000	.0000	.0000	.0000	.0000	.0000	.0000	.0000	.0000	.0000	.0000
3.16E-07	2.7602	.0000	.0000	.0000	.0000	.0000	.0000	.0000	.0000	.0000	.0000	.0000	.0000
1.00E-06	12.5547	.0000	.0000	.0000	.0000	.0000	.0000	.0000	.0000	.0000	.0000	.0000	.0000
3.16E-06	323.0181	.0067	.0068	.0069	.0006	.0006	.0004	.0004	.0001	.0000	.0000	.0000	.0000
1.00E-05	6421.7548	1.8611	1.9101	1.9656	.1239	.1368	.0760	.0760	.0036	.0039	.0037	.0030	.0029
3.16E-05		16.1965	16.6883	17.2698	1.3006	1.5314	.5432	.5506	.0693	.0981	.0980	.0943	.0946
1.00E-04		46.6051	48.2640	50.3213	4.6423	5.8311	2.4739	2.7091	1.6327	2.4717	2.4935	2.4872	2.5063
3.16E-04		98.8814	102.8798	108.0215	11.7947	15.4055	7.9948	9.0282	7.0600	10.7316	10.8320	10.8226	10.9081
1.00E-03		196.9842	205.3764	216.3112	25.3978	33.5603	18.5458	21.0806	17.2798	26.2781	26.5335	26.5171	26.7348
3.16E-03		382.3438	398.9921	420.7957	51.2494	67.9015	38.5174	43.8302	36.2192	55.0724	55.6293	55.5960	56.0735
1.00E-02		732.9663	765.1087	807.2664	100.3441	132.7612	76.1869	86.5993	71.0478	107.9883	109.1274	109.0537	110.0376
3.16E-02					193.4803	255.0460	147.0716	166.7812	134.6797	204.5911	206.8474	206.6775	208.6419
1.00E-01					360.5021	470.2504	265.8404	299.5964	231.3634	351.1008	355.1643	354.7349	358.3079
3.16E-01					629.1432	804.6558	434.3733	483.3651	337.8490	511.7038	517.9132	516.7518	522.2789
1.00E+00					959.7633		628.7843	689.0370	419.3211	633.2845	641.2753	638.5199	645.7178
3.16E+00							774.1776	839.0564	455.7589	686.2614	695.1540	690.2528	698.3236
1.00E+01							869.4852	936.0915	472.3897	709.0519	718.5906	711.4470	720.1533

TAU	1527.2+	1600.0-	1683.3-	1683.3+	1699.9-	1700.1+	1800.0	1950.0	2077.5-	2077.6+	2300.0	2516.0-	2518.0+
1.00E-05	.0006	.0005	.0005	.0002	.0002	.0002	.0001	.0001	.0001	.0001	.0000	.0000	.0000
3.16E-05	.0097	.0087	.0094	.0014	.0014	.0011	.0009	.0006	.0004	.0003	.0002	.0002	.0001
1.00E-04	.2007	.1655	.1837	.0135	.0136	.0056	.0054	.0044	.0026	.0008	.0007	.0010	.0003
3.16E-04	.9031	.7062	.7788	.0590	.0598	.0199	.0204	.0174	.0112	.0019	.0020	.0040	.0007
1.00E-03	2.2843	1.7845	1.9678	.1539	.1559	.0506	.0527	.0455	.0299	.0040	.0048	.0109	.0016
3.16E-03	4.9475	3.9031	4.3121	.3488	.3512	.1167	.1211	.1054	.0698	.0086	.0114	.0271	.0036
1.00E-02	10.0413	8.0372	8.9067	.7499	.7472	.2596	.2657	.2325	.1545	.0190	.0266	.0647	.0088
3.16E-02	19.7286	16.0556	17.8699	1.5873	1.5535	.5747	.5716	.5015	.3338	.0433	.0627	.1524	.0224
1.00E-01	35.0159	29.2803	32.8606	3.1203	2.9492	1.2136	1.1381	.9952	.6518	.1033	.1441	.3338	.0613
3.16E-01	53.0317	45.6996	51.9643	5.6089	4.9828	2.3946	2.0320	1.7494	1.1349	.2595	.3275	.6735	.1802
1.00E+00	68.6176	60.4689	69.8279	9.0757	7.5583	4.2455	3.2901	2.7896	1.8876	.6806	.7889	1.3534	.5783
3.16E+00	77.2112	68.9107	80.3216	12.3393	10.0957	6.4009	5.0011	4.4124	3.4118	1.9794	2.2963	3.2494	2.2195
1.00E+01	83.5814	75.5314	88.3139	17.1225	14.5246	10.6453	9.3541	9.3227	8.8439	7.2683	8.8730	11.4026	10.1656

TAU	2665.0	2885.0	3000.0	3200.0	3400.0	3647.1-	3647.1+	3800.0	4000.0	4200.0	4400.0	4600.0	4800.0
1.00E-05	.0000	.0000	.0000	.0000	.0000	.0000	.0000	.0000	.0000	.0000	.0000	.0000	.0000
3.16E-05	.0001	.0001	.0001	.0001	.0001	.0001	.0000	.0000	.0000	.0000	.0000	.0000	.0000
1.00E-04	.0003	.0002	.0002	.0002	.0002	.0002	.0001	.0001	.0001	.0001	.0001	.0001	.0001
3.16E-04	.0006	.0005	.0005	.0004	.0004	.0004	.0004	.0004	.0003	.0003	.0003	.0003	.0003
1.00E-03	.0014	.0012	.0011	.0010	.0010	.0011	.0010	.0010	.0009	.0009	.0010	.0010	.0010
3.16E-03	.0033	.0029	.0029	.0028	.0029	.0030	.0030	.0030	.0029	.0029	.0030	.0030	.0031
1.00E-02	.0082	.0078	.0078	.0080	.0083	.0089	.0089	.0091	.0087	.0089	.0092	.0095	.0099
3.16E-02	.0218	.0218	.0222	.0233	.0248	.0269	.0267	.0277	.0270	.0278	.0289	.0300	.0312
1.00E-01	.0618	.0638	.0659	.0705	.0758	.0831	.0818	.0855	.0840	.0871	.0906	.0944	.0983
3.16E-01	.1865	.1969	.2055	.2223	.2409	.2653	.2525	.2649	.2626	.2735	.2853	.2975	.3099
1.00E+00	.6117	.6508	.6954	.7602	.8304	.9209	.7799	.8190	.8228	.8596	.8981	.9373	.9768
3.16E+00	2.4230	2.7422	2.9353	3.2951	3.6866	4.2055	2.3804	2.5002	2.5558	2.6820	2.8112	2.9411	3.0706
1.00E+01	11.4646	13.5954	14.8317	17.1557	19.7100	23.1737	7.0350	7.4188	7.7317	8.1868	8.6524	9.1238	9.5987

TAU	5000.0	5500.0	6000.0	7000.0	8000.0	10000.0	14000.0	16500.0	25000.0	50000.0	100000.0	200000.0	500000.0
1.00E-06	.0000	.0000	.0000	.0000	.0000	.0000	.0000	.0000	.0000	.0000	.0000	.0000	.0001
3.16E-06	.0000	.0000	.0000	.0000	.0000	.0000	.0000	.0000	.0000	.0000	.0000	.0001	.0005
1.00E-05	.0000	.0000	.0000	.0000	.0000	.0000	.0000	.0000	.0000	.0000	.0001	.0003	.0019
3.16E-05	.0000	.0000	.0000	.0000	.0000	.0000	.0000	.0000	.0000	.0001	.0002	.0008	.0054
1.00E-04	.0001	.0001	.0001	.0001	.0001	.0001	.0000	.0000	.0000	.0001	.0005	.0021	.0133
3.16E-04	.0003	.0003	.0003	.0004	.0004	.0003	.0002	.0002	.0001	.0004	.0015	.0060	.0377
1.00E-03	.0010	.0011	.0012	.0012	.0012	.0010	.0005	.0002	.0003	.0013	.0051	.0203	.1263
3.16E-03	.0032	.0033	.0035	.0039	.0040	.0038	.0017	.0005	.0012	.0045	.0179	.0712	.4437
1.00E-02	.0100	.0107	.0114	.0124	.0130	.0123	.0056	.0019	.0042	.0161	.0636	.2527	1.5742
3.16E-02	.0316	.0340	.0362	.0397	.0415	.0393	.0183	.0068	.0148	.0573	.2260	.8988	5.5994
1.00E-01	.1000	.1078	.1152	.1264	.1322	.1254	.0604	.0252	.0551	.2128	.8400	3.3406	20.8123
3.16E-01	.3161	.3419	.3654	.4013	.4199	.3990	.2033	.1008	.2189	.8434	3.3273	13.2322	82.4631
1.00E+00	.9998	1.0829	1.1581	1.2733	1.3352	1.2694	.7132	.4329	.9294	3.5574	14.0335	55.8494	348.7299
3.16E+00	3.1616	3.4468	3.7076	4.1354	4.4234	4.1164	2.9093	2.2398	4.7692	18.1954	72.6047	291.0868	
1.00E+01	9.9971	11.1549	12.2805	14.4409	16.4599	14.1720	14.8803	13.4500	28.6358	109.8344	455.9122		

TAU	100.0	200.0	300.0	500.0	1000.0	2000.0	5000.0	10000.0
1.00E-08	.0000	.0000	.0000	.0000	.0000	.0000	.0000	.0000
3.16E-08	.0000	.0000	.0001	.0002	.0009	.0040	.0283	.1252
1.00E-07	.0000	.0001	.0003	.0009	.0041	.0182	.1306	.5779
3.16E-07	.0001	.0005	.0013	.0038	.0170	.0755	.5413	2.3955
1.00E-06	.0005	.0023	.0056	.0167	.0743	.3302	2.3681	10.4845
3.16E-06	.0021	.0091	.0217	.0651	.2883	1.2770	9.1182	40.2579
1.00E-05	.0080	.0337	.0783	.2270	.9658	4.1184	28.0892	120.1878
3.16E-05	.0219	.0894	.2041	.5782	2.3799	9.8164	64.1160	265.6403
1.00E-04	.0534	.2154	.4875	1.3652	5.5280	22.4117	142.8370	580.5731
3.16E-04	.1512	.6065	1.3673	3.8088	15.3014	61.5033	387.1548	
1.00E-03	.5050	2.0208	4.5490	12.6455	50.6451	202.8726		
3.16E-03	1.7731	7.0907	15.9543	44.3229	177.3440	709.6533		
1.00E-02	6.2906	25.1517	56.5851	157.1733	628.7134			
3.16E-02	22.3753	89.4601	201.2583	559.0033				
1.00E-01	83.1690	332.5375	748.1311					
3.16E-01	329.6378							
1.00E+00								
3.16E+00								
1.00E+01								

BRIGHTNESS TEMPERATURES

910.0	6464	1683.3	4314	3400.0	6483	14000.0	6428
912.0	5623	1683.3	4797	3647.1	6385	16500.0	6735
1000.0	5617	1699.9	4838	3647.1	6646	25000.0	6229
1099.0	5612	1700.1	5441	3800.0	6587	50000.0	5560
1100.0	5146	1800.0	5714	4000.0	6559	100000.0	5107
1196.0	5145	1950.0	5881	4200.0	6503	200000.0	4799
1198.0	5020	2077.5	6263	4400.0	6451	500000.0	4551
1238.0	5009	2077.6	7041	4600.0	6402	1000000.0	4426
1239.0	4488	2300.0	6843	4800.0	6357	2000000.0	4386
1350.0	4518	2516.0	6350	5000.0	6327	3000000.0	4471
1443.0	4503	2518.0	6918	5500.0	6242	5000000.0	4801
1444.0	4493	2665.0	6834	6000.0	6175	10000000.0	5700
1527.2	4484	2885.0	6725	7000.0	6081	20000000.0	6776
1527.2	4305	3000.0	6667	8000.0	6031	50000000.0	7847
1480.0	4324	3200.0	6571	10000.0	6051	100000000.0	8278

The FORTRAN versions of the key opacity routines are appended to the article by Carbon and Gingerich (1969) – AVMETS is here changed as indicated in the preceding section – and certain additional ultraviolet-opacity routines are reproduced here as Table III.

The columns of Table IV are self-explanatory; the appearance of the letter 'C' in the penultimate column indicates that the model is convectively unstable according to the Schwarzschild criterion. The columns of Table V should also be obvious after the explanation in the preceding paragraphs. Note that in Table VI there are *two* columns for each wavelength; the first gives the specific intensity per unit frequency, that is, in ergs cm^{-2} sec^{-1} Hz^{-1} $ster^{-1}$, whereas the second gives Φ, the intensity ratio with respect to the center ($\mu=1$), except for the initial number, which is the monochromatic specific intensity *per unit wavelength*, that is, in ergs cm^{-3} $ster^{-1}$ sec^{-1}. Toward the end of Table VI, the long wavelengths are designated in microns instead of angstroms. Finally, Table VII gives the monochromatic optical depths with respect to 5000 Å, as well as brightness temperatures. (The tabulated equivalence at 5000 Å itself is not exact because electron scattering has been omitted in calculating the optical depths in Table VII.)

Acknowledgements

We wish to thank Drs. W. Parkinson and E. M. Reeves for placing numerous observations at our disposal and for many discussions on problems of the solar ultraviolet. We also gratefully acknowledge the discussions with and assistance from Dr. E. H. Avrett and Mr. Duane Carbon. One of us (Y. C.) acknowledges support from the National Aeronautics and Space Administration through contract NASw-184.

References

Athay, R. G.: 1969, *Solar Phys.* **9**, 51.
Bonnet, R. M.: 1968, *Ann. Astrophys.* **31**, 597.
Bötticher, W.: 1958, *Z. Physik* **150**, 336.
Carbon, D. F. and Gingerich, O.: 1969, in *Theory and Observations of Normal Stellar Atmospheres* (ed. by O. Gingerich), Massachusetts Institute of Technology Press, Cambridge, p. 377.
Carbon, D. F., Gingerich, O., and Kurucz, R.: 1968, *Solar Phys.* **3**, 55.
Conneely, M. J., Smith, K., and Lipsky, L.: 1970, *J. Phys. B* **3**, 493.
Cuny, Y.: 1969, in *Theory and Observations of Normal Stellar Atmospheres* (ed. by O. Gingerich), Massachusetts Institute of Technology Press, Cambridge, p. 173.
Cuny, Y.: 1971, *Solar Phys.* **16**, 293.
Doyle, R. O.: 1968, *Astrophys. J.* **153**, 987.
Eddy, J. A., Léna, P. J., and MacQueen, R. M.: 1969a, *Bull. Am. Astron. Soc.* **1**, 275.
Eddy, J. A., Léna, P. J., and MacQueen, R. M.: 1969b, *Solar Phys.* **10**, 330.
Elste, G.: 1968, *Solar Phys.* **3**, 106.
Garz, T., Holweger, H., Kock, M., and Richter, J.: 1969, *Astron. Astrophys.* **2**, 446.
Gay, J.: 1970, *Astron. Astrophys.* **6**, 327.
Gingerich, O.: 1970, in L. Houziaux and H. E. Butler (eds.), 'Ultraviolet Stellar Spectra and Related Ground-Based Observations', *IAU Symp.* **36**, 140.
Gingerich, O. and de Jager, C.: 1968, *Solar Phys.* **3**, 5.
Goldberg, L., Noyes, R. W., Parkinson, W. H., Reeves, E. M., and Withbroe, G. L.: 1968, *Science* **162**, 95.

Henze, Jr., W.: 1969, *Solar Phys.* **9**, 65.
Holweger, H.: 1970, *Astron. Astrophys.* **4**, 11.
Houtgast, J.: 1968, *Solar Phys.* **3**, 47.
Koutchmy, S. and Peyturaux, R.: 1968, *Compt. Rend.* **267**, 905.
Kozlov, M. G. and Startsev, G. P.: 1969, *Opt. Spectrosc.* **27**, 383.
Labs, D. and Neckel, H.: 1968, *Z. Astrophys.* **69**, 1.
Labs, D. and Neckel, H.: 1970, *Solar Phys.* **15**, 79.
Lambert, D. L. and Warner, B.: 1968, *Monthly Notices Roy. Astron. Soc. London* **138**, 181.
Léna, P. J.: 1970, *Astron. Astrophys.* **4**, 207.
Linsky, J. and Avrett, E. H.: 1970, *Publ. Astron. Soc. Pacific* **82**, 169.
Mankin, W. G.: 1969, Ph.D. Thesis, Johns Hopkins University, Baltimore, Md.
Mankin, W. G. and Strong, J.: 1969, *Bull. Am. Astron. Soc.* **1**, 200.
McGuire, E. J.: 1968, *Phys. Rev.* **175**, 20.
Noyes, R. W. and Kalkofen, W.: 1970, *Solar Phys.* **15**, 120.
Parkinson, W. H. and Reeves, E. M.: 1969, *Solar Phys.* **10**, 342.
Parkinson, W. H. and Reeves, E. M.: 1970, Personal communication.
Peach, G.: 1967, *Mem. Roy. Astron. Soc.* **71**, 29.
Saiedy, F.: 1960, *Monthly Notices Roy. Astron. Soc. London* **121**, 483.
Sando, K.: 1969, Personal communication (see Table III).
Sando, K., Doyle, R. O., and Dalgarno, A.: 1969, *Astrophys. J.* **157**, L143.
Tousey, R.: 1963, *Space Sci. Rev.* **2**, 3.
Widing, K. G., Purcell, J. D., and Sandlin, G. D.: 1970, *Solar Phys.* **12**, 52.